JOURNAL OF QUATERNARY SCIENCE (2002) **17**(5-6) 491–510

Published online in Wiley InterScience (www.interscience.wiley.com). DOI: 10.1002/jqs.713

Global glacial isostatic adjustment: palaeogeodetic and space-geodetic tests of the ICE-4G (VM2) model

W. R. PELTIER*

Department of Physics, University of Toronto, Toronto, Ontario M5S 1A7, Canada

Peltier, W. R. 2002. Global glacial isostatic adjustment: palaeogeodetic and space-geodetic tests of the ICE-4G (VM2) model. *J. Quaternary Sci.,* **Vol. 17** pp. 491–510. ISSN 0267-8179.

Received 10 January 2002; Revised 25 June 2002; Accepted 3 July 2002

ABSTRACT: Analyses of the global process of glacial isostatic adjustment and post-glacial relative sea-level change continue to deliver important insights into Earth system form and process. One successful model of the related phenomenology is based upon a spherically symmetric internal viscoelastic structure for the solid Earth, which has been denoted VM2, and a model of the most recent deglaciation event of the current ice-age, denoted ICE-4G. The primary purpose of this paper is to describe several new *a posteriori* tests that have recently been performed to further investigate the quality of this global 'solution' to the inverse problem for both mantle viscosity and deglaciation history that is posed by the observables associated with this large-scale geodynamic phenomenon. I focus especially upon the 'misfits' of observations to the theoretical predictions of this model, which I am currently using to further refine its properties, and upon predictions made using it of geophysical signals that should soon become visible in the context of the Gravity Recovery and Climate Experiment (GRACE) satellite mission. Among the required refinements to ICE-4G, one that is necessary to eliminate a recently revealed misfit to space geodetic constraints on the present-day rate of radial motion at the Yellowknife location well to the west of Hudson Bay, and a similar misfit to absolute gravity measurements to the southwest of the Bay, is the insertion of a 'Keewatin Dome' of thick ice centred over Yellowknife with a ridge of ice extending to the south east. In the geomorphological literature, the existence of such a Keewatin Dome previously has been hypothesised but chronological control was lacking on the surface features that suggested its former existence. An important additional constraint that requires the late glacial existence of this important feature consists of new inferences of the Last Glacial Maximum lowstand of the sea from sites in the far field of the main concentrations of land ice. Copyright © 2002 John Wiley & Sons, Ltd.

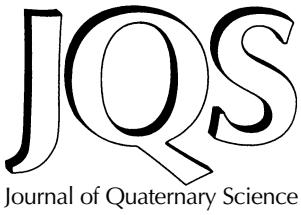

KEYWORDS: Laurentide Ice Sheet; geodetic constraints; Keewatin; glacial isostasy; mantle viscosity; earth rotation; sea level history.

Introduction

The basis of the modern viscoelastic normal-mode-based field theory that currently serves as standard for analysis of the suite of interconnected geological–geophysical–astronomical observations related to the glacial isostatic adjustment process was established in Peltier (1974). It was demonstrated therein how one could use Laplace transform methods to extend the analysis of Farrell (1972) of the surface loading problem for a spherically symmetric elastic model of Earth to the case of a spherically symmetric viscoelastic model in which the viscoelasticity was described using a linear Maxwell rheology. The choice of the Maxwell model was argued therein as being required in order that the rheology of the mantle be asymptotically correct in both the long-timescale and short-timescale limits, Hookean elastic in the latter case and Newtonian viscous in the former. That the long-timescale behaviour should be viscous (although not necessarily Newtonian) is clearly required in order that continental drift and sea-floor spreading be explicable in terms of the fluid mechanical process of thermal convection. The issue as to whether the viscous fluid flow of the mantle of Earth occurs via a Newtonian process as opposed to a non-Newtonian creep mechanism remains largely unresolved. Arguments recently have been presented on both sides of this debate (e.g. Forte and Mitrovica, 1996, 2001; Peltier, 1996a; Wu, 1998, 1999; Butler and Peltier, 2000, 2001) but no definitive result has yet been obtained. Similarly outstanding is the question as to whether the influence of lateral viscosity heterogeneity is significant and whether, if it is significant, its influence may be adequately described using first-order perturbation theory (e.g. Tromp and Mitrovica, 1999) or whether more demanding non-perturbative methods (e.g. Wu *et al.*, 1998; Martinec, 2000) will in fact be required. Regardless of the answers to these important outstanding questions, the existing linearly viscoelastic and spherically

*Correspondence to: W. R. Peltier, Department of Physics, University of Toronto, Toronto, Ontario M5S 1A7, Canada.

symmetric field theory has so clearly demonstrated its capacity to reconcile the vast majority of the observations that it will continue to serve for the foreseeable future as the primary vehicle for their interpretation.

Although it is not my purpose here to provide a detailed recapitulation of this theoretical structure, as a very comprehensive recent review will be found in Peltier (1998a), it is nevertheless important to enumerate the set of physical effects that the theory has been designed to incorporate so that one might better understand what may be missing. Basic to the theory is a detailed computation of the viscoelastic response of a spherically symmetric model of the planet to the changing surface mass load that accompanies the glaciation–deglaciation process, as water is removed from the oceans to build the ice sheets and then returned to the oceans when they disintegrate. As the ocean loading–unloading component of surface mass load history must be determined from the assumed known history of ice unloading–loading, this computation requires the solution of an integral equation (to which I refer as the sea-level equation, SLE) that uses a kernel (Green function) for the separation between the geoid and the surface of the solid Earth caused by a shift in surface load (Peltier and Andrews, 1976; Farrell and Clark, 1976).

Because there is a significant response of Earth's rotational state to the glaciation–deglaciation process, once the integral SLE has been solved to determine the complete history of surface loading one may then proceed to solve the appropriate Euler equation (Peltier, 1982; Wu and Peltier, 1984) to determine the rotational response and compare this to astronomical observations of the non-tidal acceleration of planetary rotation (or equivalently $\dot{J}_2$, a quantity proportional to the time rate of change of the degree 2 and order zero Stokes coefficient in the spherical harmonic expansion of the gravitational potential of the planet) and the speed and direction of the ongoing 'wander' of the pole of rotation with respect to the surface geography. As these rotational responses to the glaciation–deglaciation process both feed-back on to sea level, the SLE must be modified to incorporate this effect. The results of Dahlen (1976) have proven to be important in this regard (Peltier, 1998a; Peltier, 1999). Recently published detailed analyses of this feed-back (Peltier, 1998a, 1999) have demonstrated that its influence is usually weak on relative sea-level (RSL) history insofar as Holocene records are concerned, although there do exist regions, as discussed in what follows, where this influence is important. Also to be discussed in what follows, moreover, and as demonstrated in Peltier (1999), this feed-back is not negligible upon the time rate of change of sea-level when this is referenced to the centre of mass of Earth rather than to the surface of the solid Earth. As the GRACE (Gravity Recovery and Climate Experiment) mission will provide a global map of just this geoid height time dependence, it will be important in the analysis of these data that the influence of rotational feed-back be carefully included.

It has also proven possible to fully incorporate into this theory the influence on relative sea-level history of the migration of the land–sea interface (by exploiting the fact that the first-order perturbation theoretic form of the SLE predicts sea-level history relative to an arbitrary and thus unspecified datum; Peltier, 1994). However, the nature of this influence is such that we are then obliged to recognise the fact that the ice-unloading history that we specify as input to the solution of the integral SLE, in the course of tuning it to fit near-field rebound observations, becomes an 'effective' unloading history that we must later recognise to have been augmented by the action of 'implicit ice' (Peltier, 1998b) in consequence of the action of the dramatic changes in land–sea distribution that occur when initially ice-covered inland seas such as Hudson Bay, the Gulf of Bothnia and the Barents and Kara Seas become connected to the oceans. The influence of ocean function time dependence may also introduce significant impact in the far field of the ice sheets in regions where a broad continental shelf is significantly exposed by the fall of sea-level that attends the time of maximum continental glaciation (Peltier and Drummond, 2002; Peltier, 2002a,b).

In the context of a spherically symmetric linear viscoelastic model of Earth, the existing field theory is therefore rather complete. One of the things we expect to learn by exercising it, through comparison of its predictions to the observations, is whether these primary assumptions must eventually be abandoned. Unless we are able to identify a sequence of systematic misfits of the theory to the observations, we will clearly not be able to resolve the asphericity of viscosity that certainly must exist on some (perhaps small) horizontal spatial scale in the convecting mantle and/or the deviation from Newtonian behaviour that might be expected on apriori grounds to govern the creep of the polycrystalline mantle of Earth (see e.g. Wu (1999) for a recent discussion).

Theoretical structure: tuning the model inputs and far-field tests of ICE-4G (VM2)

The form of the SLE that incorporates all of the physical interactions enumerated above may be expressed as

$$S(\theta,\lambda,t) = \left[\int_{-\infty}^{t} \mathrm{d}t' \iint_{\Omega} \mathrm{d}\Omega' \left\{ L(\theta',\lambda',t') G_{\phi}^{L}(r-r',t-t') + T(\theta',\lambda',t') G_{\phi}^{T}(r-r',t-t') \right\} + \frac{\Delta\Phi(t)}{g} \right] \times C(\theta,\lambda,t) \quad (1)$$

In this equation, S is the change in the mean level of the sea (the geoid) relative to the deforming surface of the solid Earth, C is the so-called 'ocean function', which is unity over the oceans and zero over the continents, Ω is the surface of the Earth on which θ is latitude and λ is longitude, and L is the space and time-dependent surface mass load per unit area, which has the composite structure

$$L(\theta,\lambda,t) = \rho_{\mathrm{I}} I(\theta,\lambda,t) + \rho_{\mathrm{w}} S(\theta,\lambda,t) \quad (2)$$

In equation (2) ρ_{I} and I are ice-density and thickness, respectively, and ρ_{w} and S are ocean density and relative sea-level change respectively. The function T in equation (1), which is analogous to L, is the change in the centrifugal potential forcing that both the surface of the ocean and the solid Earth will feel because of the changes in Earth rotation induced by the glaciation–deglaciation process. The functions G_{ϕ}^{L} and G_{ϕ}^{T} are the Green functions for the separation between the geoid and the surface of the solid Earth associated respectively with surface mass loading and tidal (centrifugal potential) loading, and the time dependent function $\Delta\Phi(t)$ must be constructed such that the post-glacial sea-level history obtained by solving the SLE (1) is mass conserving in the sense that only the mass lost by melting ice increments the total volume of the oceans. As the understanding of the importance of this term will be crucial to understanding the results of one of the tests of the ICE-4G (VM2) model to be described, it will be worthwhile to recapitulate its derivation here. Multiplying

equation (1) by the density of ocean water ρ_w and integrating over the ocean basins it will be clear that

$$\iint_{\Omega_o} \rho_w S \mathrm{d}\Omega = \rho_w \iint_{\Omega_o} Z \mathrm{d}\Omega + \rho_w \frac{\Delta\Phi(t)}{g} \iint_{\Omega_o} \mathrm{d}\Omega \quad (3)$$

where Ω_o is the surface of the oceans and Z is the triple convolution integral in equation (1). Now conservation of mass clearly requires that

$$\iint_{\Omega_o} \rho_w S \mathrm{d}\Omega = M_I(t) \quad (4)$$

where $M_I(t)$ is the mass of continental ice lost as a result of melting by time t. It therefore follows that

$$\frac{\Delta\Phi(t)}{g} = \frac{M_I(t)}{\rho_w A_o(t)} - \frac{1}{A_o(t)} \iint_{\Omega_o} Z \mathrm{d}\Omega \quad (5)$$

The first term on the right-hand side of equation (5) is just the eustatic sea-level history, $S_{eus}(t)$ say, where $A_o(t)$ is the time-dependent surface area of the oceans, i.e.

$$S_{eus}(t) = \frac{M_I(t)}{\rho_w A_o(t)} \quad (6)$$

Substituting equation (5) into (1) we may therefore rewrite this most general form of the SLE so as to fully account for the action of implicit ice (see Peltier (2002a) for further discussion) as

$$S = [Z - \langle Z \rangle + S_{eus}(t) - S^{im}_{eus}(t)] C(\theta, \lambda, t) \quad (7)$$

in which $\langle Z \rangle$ is the (time dependent) average value of the triple convolution integral in equation (1) over the time varying surface area of the oceans and $S^{im}_{eus}(t)$ is the 'implicit' component of the ice load that is activated by the time dependence of the ocean function in the regions of continental deglaciation that later come to be inundated by the sea.

The mathematical method used to solve equation (1) is iterative and makes use of the fact that both the influence of migration of the land–sea interface that is expressed in the time dependence of C and the influence of rotational feedback on to sea-level that is expressed through the convolution of T with G^T_ϕ are second-order effects. The complete algorithm recently has been reviewed in Peltier (1998a), an important component of which is a significantly modified version of the semi-spectral methodology (Mitrovica and Peltier, 1991) that is now used to solve the SLE in the absence of these influences.

Now the inputs to equation (1) consist of the deglaciation history $I(\theta, \lambda, t)$ and a model of the radial viscoelastic structure of Earth, the latter requiring the specification of the density $\rho(r)$, the two elastic Lamé parameters $\lambda(r)$ and $\mu(r)$, and the viscosity $\nu(r)$. I continue to use the PREM model of Dziewonski and Anderson (1981) to fix the first three of these parameters on the basis of seismic observations. The remaining parameter $\nu(r)$ is then fixed by formal (perhaps Bayesian) inversion of a subset of the glacial isostatic adjustment observations that are expected to be essentially independent of any error that might be associated with the specification of $I(\theta, \lambda, t)$ (see Peltier and Jiang (1996), Peltier (1996a) and Peltier (1998d) for detailed recent discussions of the various models $\nu(r)$ that have been determined in this way). Figure 1 shows three examples of such models, which are respectively labelled VM1, VM2 and VM3. Models VM2 and VM3 were derived on the basis of Bayesian inversions in which the VM1 model of Tushingham and Peltier (1991, 1992) was used as a starting model. The data used to drive the refinement of VM1 consisted of 23 site-dependent relaxation times from Canada and Fennoscandia, the relaxation time spectrum of McConnell (1968) for the rebound of Fennoscandia (recently reanalysed by Wieczerkowski *et al.* (1999) who infer a flatter spectrum at short wavelength, implying a somewhat thinner lithosphere, and somewhat higher relaxation times at long wavelength, implying somewhat higher viscosity at depth) and the observed non-tidal acceleration of planetary rotation. As

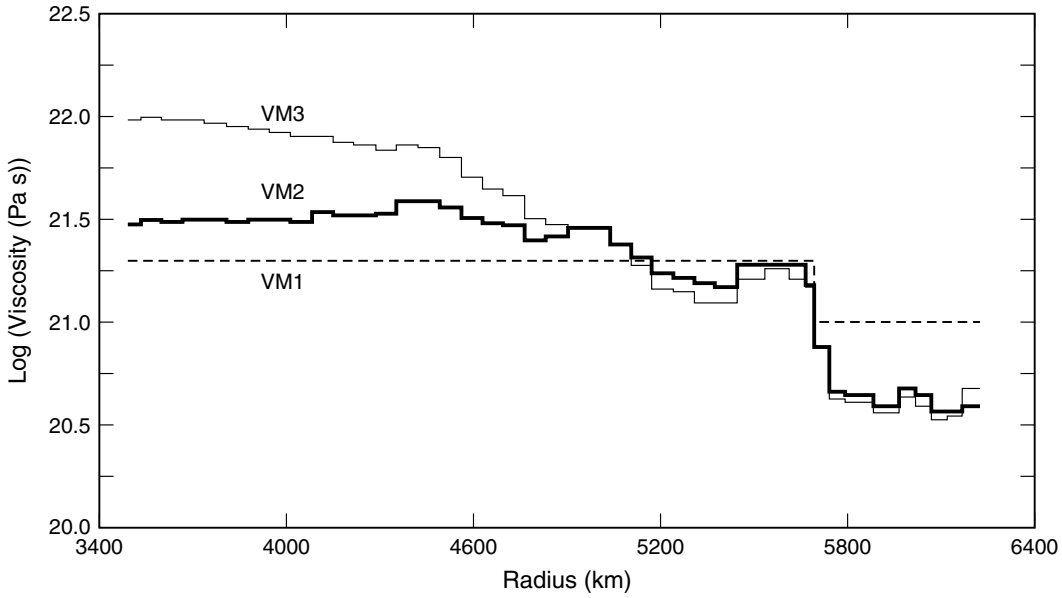

Figure 1 Example of radial profiles of mantle viscosity that have arisen in the context of inversions of observations related to the glacial isostatic adjustment process. The profile labelled VM1 is a simple four-layer profile suggested by trial and error fits to a large set of ^{14}C dated RSL observations in Tushingham and Peltier(1990). Profile VM2 is the model obtained in Peltier and Jiang (1996) and Peltier (1996),who used the method of Bayesian inference described in detail in Tarantola and Valette (1982), with VM1 as a first guess, to invert a set of 23 site-specific relaxation times from Canada and Fennoscandia, together with the Fennoscandianrelaxation spectrum of McConnell (1968) and the observed non-tidal acceleration of planetary rotation. Profile VM3 was obtained by adjusting the non-tidal acceleration of rotation observation so as to allow for the possible influence of contamination owing to significant present-day melting of the Greenland and/or Antarctic ice-sheets

shown in Peltier (1996a), the VM2 model determined in this formal way entirely eliminated the gross misfits between RSL observations and the predictions made using the VM1 viscosity model that previously had been identified by Tushingham and Peltier (1992) at sites along the east coast of the continental USA. The VM3 model shown on Fig. 1 differs from VM2 only in the deepest part of the lower mantle and was obtained in a Bayesian inversion in which it was assumed that the observed non-tidal acceleration was significantly contaminated by present-day melting of the Greenland and/or Antarctic ice-sheets, which were assumed to be causing eustatic sea-level to be rising at the rate of 1.5 mm yr^{-1} (see Douglas and Peltier (2002) for a recent discussion of possible sources). As currently there exists no unequivocal evidence that such a significant rate of eustatic rise resulting from the present-day melting of these polar ice-sheets is occurring, it should be clear that the VM3 model with highest lower mantle viscosity must be considered tentative.

Of extreme, perhaps most extreme, importance, insofar as the inputs to equation (1) are concerned, is the global deglaciation history embodied in the space- and time-dependent function $I(\theta, \lambda, t)$. In the absence of rather tight apriori constraints upon this function, the problem of model development would be even more formidable than it is now. Over the past 50 yr, however, the efforts of the international community of geomorphologists have led to rather clear definition of the regions on the surface of the planet that were most heavily glaciated at Last Glacial Maximum ca. 21 000 cal. yr BP and, through ^{14}C dating of the terminal moraines constructed during ice-sheet retreat, to an equally clear definition of the chronology of the deglaciation process (e.g. see Dyke *et al.* (2002) for the most recent discussion of the Laurentide Ice Sheet and other papers in the January 2002 issue of *Quaternary Science Reviews* for discussions of other glaciated regions). When coupled with the recently obtained high-quality constraints on the time-dependent net rise of sea-level from LGM to present that is embodied in the U/Th dated coral record from the island of Barbados (Fairbanks, 1989; Bard *et al.*, 1990), this data set enables us, to a large degree, to disconnect the cross-propagation of error between the imperfectly known parameters of the model, namely $I(\theta, \lambda, t)$ and $\nu(r)$. Figure 2a shows a detailed intercomparison between the prediction of

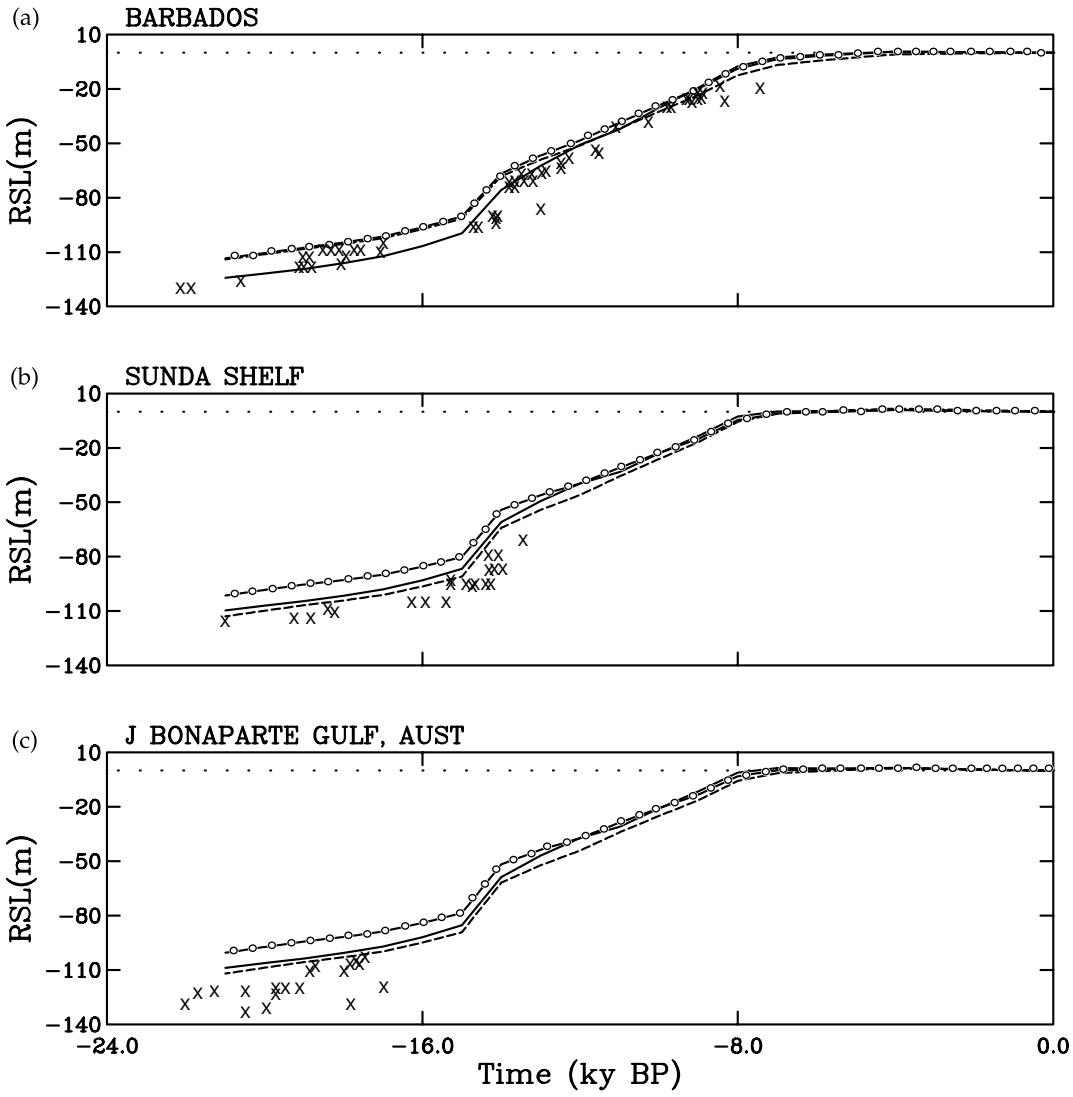

Figure 2 (a) Predicted relative sea-level histories for the ICE-4G model of deglaciation (∘-∘-∘-∘-∘) and for the ICE-5GP (VM2) model discussed in the text (———) along with the observations from the Island of Barbados (after Fairbanks, 1989; Bard *et al.*, 1990) on the calendar year time-scale and corrected for an assumed rate of tectonic uplift of .34 mm yr^{-1}. Also shown is the prediction (- - - -) for the ICE-4G model in which the influence of the 'broad shelf effect' is neglected. (b) Same as in (a) but for the Sunda Shelf with the observations of Hanebuth *et al.* (2000) shown for comparison purposes. (c) Same as in (a) but for J. Bonaparte Gulf with observations of Yokoyama *et al.* (2000) shown for comparison. Clearly the influence of the 'broad shelf effect' is of no importance at the Barbados location

RSL history at Barbados based upon the solution of equation (1) using essentially the ICE-4G input (dashed green lines include the influence of the 'broad shelf effect' discussed in Peltier (2002a,b) and Peltier and Drummond (2002); the version of ICE-4G being used herein is that discussed in Peltier (2002a) in which the ice equivalent net eustatic rise is 113.5 m, 4.3 m lower than in the original ICE-4G model owing to the reduction of the amount of Antarctic deglaciation by this amount) as well as a second prediction (shown as the solid black curve, which also includes the 'broad shelf effect') for a model to which I will refer as ICE-5GP, in which the LGM ice load in the North American component of ICE-4G has been enhanced significantly in the region well to the west of Hudson Bay (the letter 'P' in the label used to denote this model represents 'preliminary'; the final form of the ICE-5G model not yet being firm). The third prediction shown on Fig. 2 as the dashed red curve is for a model that uses ICE-4G melting history, does not include the 'broad shelf effect', and uses a vertical viscosity profile that is the same as VM2 except in the lower mantle, where the viscosity is elevated at all depths below 660 km to the value of 10^{22} Pa s, the value of this Earth property preferred by Lambeck and colleagues (e.g. Lambeck *et al.*, 1990, 1996). The two models of the deglaciation history, ICE-4G and ICE-5GP, clearly bracket the Barbados observations, with ICE-4G apparently representing a lower bound on ice amount (as discussed in Peltier, 2002a) and the new model ICE-5GP representing an approximate upper bound. As the data from Barbados provide a good approximation to eustatic sea-level history itself (Peltier, 2002a), the lower and upper bounds on the net eustatic rise appear to be ca. 113.5 m and ca. 130 m.

Also shown, on Fig. 2b and c, are additional intercomparisons with two recently published relative sea-level records from the western equatorial Pacific Ocean, respectively from the Sunda Shelf (Hanebuth *et al.*, 2000) and from Bonaparte Gulf (Yokoyama *et al.*, 2000). As the ICE-4G deglaciation history has been tuned so as to enable the model to fit the relative sea-level record at Barbados, the fact that it fits the data from this location says nothing at all about the accuracy of the model. It is highly significant, however, that model ICE-5GP also fits these observations, emphasising the degree of non-uniqueness of the constraint upon the net eustatic rise provided by the Barbados data set. Inspection of the comparisons for the Sunda Shelf and Bonaparte Gulf sites, from which the data were not used to tune the deglaciation history, however, shows that only the ICE-5GP model of the deglaciation history fits the observations in these regions where LGM shelf exposure was extreme (Peltier, 2002a,b; Peltier and Drummond, 2002). The RSL analyses at these two additional sites demonstrate them to be very poor facsimiles of $S_{\mathrm{eus}}(t)$, unlike Barbados, a consequence of the fact that the 'broad shelf effect', recently discussed in detail in Peltier and Drummond (2002), is very significant in both of these regions.

Inspection of the raw RSL data from each of the Barbados, Sunda Shelf and Bonaparte Gulf locations, furthermore, shows that although the Barbados data would allow for the existence of a very sharp influx of meltwater to have reached the global ocean at approximately 19 000 cal. yr ago, as recently suggested by Yokoyama *et al.* (2000) based upon the Bonaparte Gulf data, the record from the Sunda Shelf appears to strongly restrict its possible magnitude. Further, more detailed discussion of these interesting issues will be found in Peltier (2002a,b). What we can say based upon these intercomparisons, however, is that the net eustatic rise that occurred during the deglaciation of the continents must have been significantly greater than the 113.5 m characteristic of the modified version of ICE-4G being used here and in Peltier (2002a). A primary focus of the discussion to follow will be on the issue as to where on the continents the large additional amount of land ice may have resided, ice that appears to be required by the new LGM data sets that derive from studies of post-LGM far-field shelf inundation. The issue of mantle viscosity will prove to be important in answering this question and so it will be useful to revisit the nature of the constraints that may be brought to bear upon this quantity.

Laurentide relaxation-time tests of the ICE-4G (VM2) model

In order to provide a further aposteriori test of the VM2 viscosity component of the ICE-4G (VM2) model than that provided by the extremely important data sets from the USA east coast mentioned previously, it proves interesting to focus further upon the Laurentide platform itself, a region that was entirely ice-covered at LGM. Figure 3a shows the locations of a large number of sites on this platform from which high quality ^{14}C dated time-series of RSL history are available, many of the best of which are from the Canadian high Arctic (Dyke and Peltier, 2001). I have determined exponential relaxation times for the uplift at each of these locations using an entirely objective Monte Carlo technique applied to time series in which the age of each sample has been calibrated to calendar year age using the Stuiver and Reimer (1993 and subsequent) CALIB procedure. These Monte Carlo fits have been determined in two ways, which differ from one another according to whether or not account is taken of the 'storm beach offset' (see discussion on p. 608 of Peltier, 1998a). The relaxation times inferred in these two ways are plotted against one another on Fig. 3b for the set of locations shown on Fig. 3a. Figures 4a and 4b respectively compare these inferred relaxation times to those predicted by the ICE-4G (VM2) model for each site. Inspection of these intercomparisons demonstrates that the model provides a reasonably good fit to the totality of the data although there is significant scatter. Furthermore, it will be clear by comparing the results shown on the two panels of Fig. 4 that the RMS misfit of the theory to the observations is not significantly influenced by correction for any storm-beach offset. The sense of the model bias is such that the centroid of the cluster of observed relaxation times lies below that of the model predictions, with a RMS relaxation time misfit of ca. 1 kyr (neglecting the single outlier). The sense of this bias suggests that the VM2 model is somewhat overly viscous over the range of depths to which the Laurentide rebound is sensitive. As data from the Laurentide platform were used in the Bayesian inversion that delivered VM2 from the starting model VM1, the existence of this bias might seem surprising. It therefore needs to be understood that the data base used for the purpose of this aposteriori check on the quality of the model is considerably different from that used in the initial Bayesian inversion and also that the calibration of the ^{14}C scale used is more accurate than that used previously (note, however, that there continues to be debate over the appropriate reservoir correction that should be applied to convert the ^{14}C age to calendar year age.

Recently there has been an entirely independent analysis performed on essentially the same set of time series (Dyke and Peltier, 2001) in an attempt to confirm the existence of the slight bias to overly long relaxation times that is suggested above to be characteristic of the VM2 model. This analysis was performed by Dyke, whose work led to the original collection of the data from most of the sites analysed, including all of the data from high Arctic locations. He did not use a method that

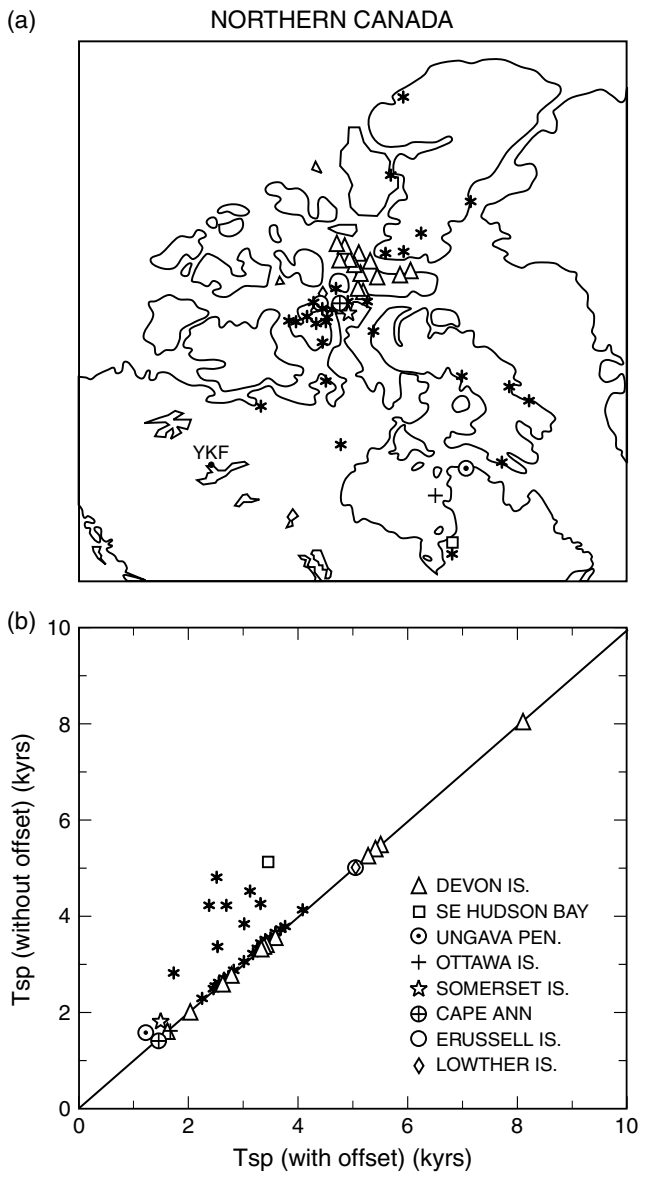

Figure 3 (a) Sites of the Laurentide platform from which high-quality ^{14}C dated RSL time series are available. (b) Exponential relaxation times inferred on the basis of 'blind' Monte Carlo fits to the RSL data at the sites shown on the location map (a). Relaxation times determined on the basis of analyses that properly correct for the 'storm beach offset' are plotted against relaxation times determined by neglecting the influence of this effect. Note that it is at a minority of these sites at which the existence of such an offset significantly modifies the inferred relaxation time

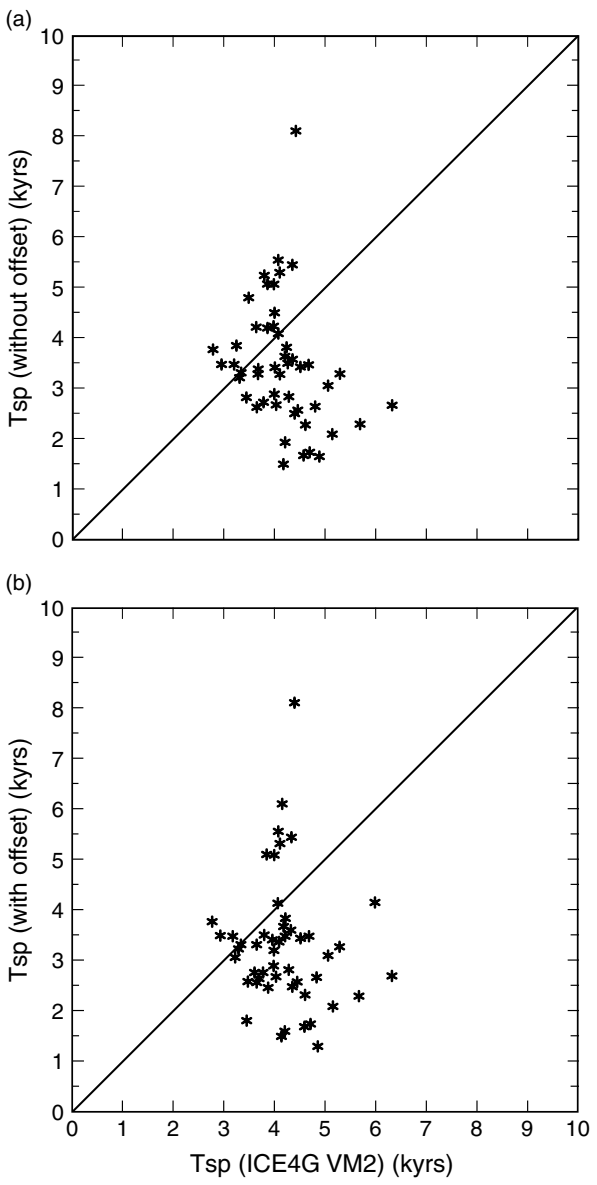

Figure 4 (a) Inferred relaxation times not corrected for the 'storm beach offset' as a function of the relaxation times predicted for the individual locations on the basis of the ICE-4G (VM2) model of the glacial isostatic adjustment process. (b) Same as in (a) but with corrections applied for the 'storm beach offset'

was constrained to produce a model exponential RSL curve which optimally passed through the data points themselves but rather made qualitative use of the understanding that the individual sea-level markers used to define the RSL curves were mostly derived from ^{14}C dated mollusc shells belonging to species whose habitat could extend to significant depth below sea level. He also strongly constrained each RSL curve to be consistent with the accurately observed and radiocarbon dated marine limit at each location, a datum not explicitly used in my own Monte Carlo analyses (except in the single case of the southeast Hudson Bay data set discussed in detail in Peltier (1998a)). A smooth curve was drawn for each data set that best respected the indicative meaning concerning RSL of each of the samples, and this curve was then best fit by a single exponential function using a least-squares method. Figure 5 shows a comparison between the relaxation time data determined in this way and the predictions of the ICE-4G (VM2) model. Inspection of Fig. 5 demonstrates that the relaxation times inferred in Dyke and Peltier (2001) are also systematically lower than the relaxation times predicted on the basis of the ICE-4G (VM2) model (note that the relaxation times reported in Dyke and Peltier were given as 'doubling times' rather than exponential relaxation times and were given on the ^{14}C scale rather than on the calendar year scale: the values shown on Fig. 5 have been converted to exponential relaxation times on the calendar year time-scale using the mapping between relaxation times on the ^{14}C time-scale and relaxation times on the calendar year time-scale provided explicitly in Peltier *et al.* (2002)). Furthermore this analysis procedure further enhances the misfits and thus reinforces the conclusion that there may be an important further modification that needs to be made to the VM2 viscosity profile.

The results shown on Fig. 5 are useful as they rather strongly suggest that the error, if any, in the VM2 viscosity model is such that the viscosity is too high over the range of depths

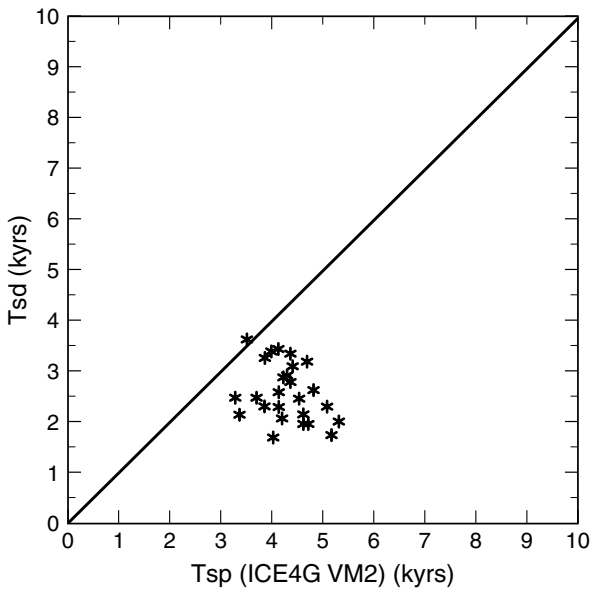

Figure 5 Inferred relaxation times from relative sea-level data at most of the site locations shown in Fig. 2a using the method of Dyke and Peltier (2000) rather than the 'blind' Monte Carlo technique used to infer the relaxation times shown on Figs 2b and 3a,b. These relaxation times are shown as a function of the relaxation times predicted by the ICE-4G (VM2) model of the glacial isostatic adjustment process. Note that these new inferences of relaxation time are lower than those delivered by 'blind' Monte Carlo inversion

to which the RSL curves from the Laurentide platform are most sensitive. As this range of depths consists primarily of the top 500–700 km of the lower mantle (e.g. see Peltier (1996a) for a typical Fréchet kernel for viscosity from a typical Laurentide platform site), if the revised Dyke and Peltier (2001) relaxation times are correct, this will require that the viscosity of this region of the upper mantle be reduced below the $1-2 \times 10^{21}$ Pa s value that is characteristic of the VM2 model. The sense of this correction is such as to even more strongly rule out the high values of lower mantle viscosity that have been proposed by a number of other groups, as these were recorded on plate 7 of Peltier (1998a). For the purpose of the present paper this demonstration that the lower mantle viscosity beneath Laurentia cannot be increased significantly, if at all, will be crucial.

Mitrovica *et al.* (2000) have recently reanalysed the complete set of ^{14}C dated RSL constraints from the southeast Hudson Bay location that were first tabulated and analysed in Peltier (1998a). The latter analysis led to the conclusion that the best estimate of the relaxation time in this region, which was near the centre of the Laurentide Ice Sheet and thus relatively immune from the influence of imprecision in our knowledge of load variations near the ice-sheet margin, was near 3.4 ka. The ICE-4G (VM2) model prediction of the relaxation time at this location is somewhat higher than this, at 4.1 ka, in accord with the above discussion, which implies that the viscosity in the upper part of the lower mantle in VM2 may be somewhat high. Mitrovica *et al.* (2000) suggest that the 3.4 ka relaxation time inferred for southeast Hudson Bay should be seen as suspect because it represents an average value for the region as a whole and because individual curves from the region may be taken to imply somewhat lower or somewhat higher relaxation times (e.g. James Bay and Richmond Gulf respectively). However, their analysis is based upon the notion that the best RSL curve must pass through rather than above the individual data points on the height versus time curve. It furthermore fails to recognise that the entire southeast Hudson Bay region was deglaciated simultaneously (Andrews and Falconer, 1969) and that the marine limit of age ca. 7.9 ka on the ^{14}C scale is now found everywhere at very nearly the same ca. 270 m elevation above present sea-level, as pointed out in Peltier (1998a). There is therefore no foundation for the argument that nearby sites in southeast Hudson Bay have been uplifted in a radically different fashion, as would be implied if the uplift at such sites were characterised by significantly different relaxation times. The notion that there existed a physically important difference between the relaxation times at closely spaced sites near the centre of Laurentide rebound was also advocated strongly by Mitrovica (1996), who suggested that models with very high lower mantle viscosity could not be ruled out by these data. This view is clearly now untenable. By combining all of the data from the southeast Hudson Bay centre of uplift we significantly increase the stability and accuracy of the inferred rate for the region as a whole. Ongoing plans to obtain an isolation basin based RSL curve from the southeast Hudson Bay region would be very helpful to the further development of a consensus view concerning the best estimate of relaxation time for this region.

As is clear on the basis of the form of the Fréchet kernels for various data from the complementary region of Fennoscandia (Peltier, 1996a), the ice sheet over this region was simply too small in areal extent for the sea-level data from it to be significantly sensitive to the viscosity structure in the upper part of the lower mantle. The relatively high value of the viscosity of the upper part of the lower mantle that is preferred by Lambeck *et al.* (1990, 1996) for this region, although it is not ruled out by the regional data, is not significantly constrained by it either. Naturally, if the new relaxation time data from Laurentia determined in Dyke and Peltier (2001) are used as constraints on the mantle viscosity inverse problem, in place of those obtained on the basis of 'blind' Monte Carlo inversion, then not only will viscosity be further reduced in the upper part of the lower mantle but the rotational constraints will require that the viscosity in the lowest part of the lower mantle be somewhat further increased, thus leading to a viscosity model of the VM3 type but one that may not rely substantially upon enhanced rotational forcing owing to the melting of polar ice for its validity. Detailed discussion of the results obtained in such further analyses of the inverse problem will be reported elsewhere.

The fact that the glacial isostatic adjustment constraints appear to require a radial variation of viscosity that is 'soft', insofar as its large length-scale averaged properties to mid-mantle depth are concerned, has recently suggested a means of making closer contact with the issue as to whether mantle viscosity is Newtonian or non-Newtonian. Butler and Peltier (2000), for example, demonstrate that when a viscosity structure such as VM3 is directly inserted into an apriori model of the mantle convection process then the convection model tends to significantly overpredict the surface heat flow. Taken at face value this has been construed to suggest either that the viscosity which controls the process of mantle convection is significantly higher than that which controls rebound (implying that the rheology of the mantle is significantly non-Newtonian), or that the extent to which the convective circulation is layered is much higher than is often assumed. Further analyses of this issue in the context of renewed considerations of planetary thermal history (Butler and Peltier, 2002) have demonstrated that this argument may be very much strengthened when the contribution to present-day heat flow as a result of the secular cooling of the planet is taken into account. Taken together, these analyses might be construed to strongly suggest that the viscosity of the mantle on the convection time-scale is significantly higher

than the viscosity on the time-scale of rebound. It is also possible, however, as mentioned in these papers, that radial heat transfer could be more significantly impeded by surface plate rigidity through an enhancement of the aspect ratio of individual convection cells, or by plate resistance, than is currently imagined. If this were the case then the Newtonian whole-mantle convection model could be resuscitated. As it stands, and especially given the most recent results from seismic tomographic imaging, which demonstrate that the 660 km seismic discontinuity resulting from the Spinel–post-Spinel phase transition often significantly impedes the progress of descending slabs, models of the convective circulation that are moderately layered and which are governed by a viscosity that is close to the rebound inferred value (Newtonian models) seem rather compelling (Peltier, 1998a).

VLBI-based tests of model predicted radial and tangential motions and the additional constraint provided by absolute gravity observations

Perhaps the most important differences in the RSL predictions of the VM1 and VM2 viscosity models are those that are evident, as previously mentioned, at sites along the east coast of the continental USA. Specifically (see fig. 23 of Peltier, 1998a), the VM1-based model dramatically overpredicts the rate of relative sea-level rise at all sites along the coast from South Carolina northwards. The VM2 model, however, rather precisely fits the data from all locations along this coast from the state of Maine south to the state of Florida.

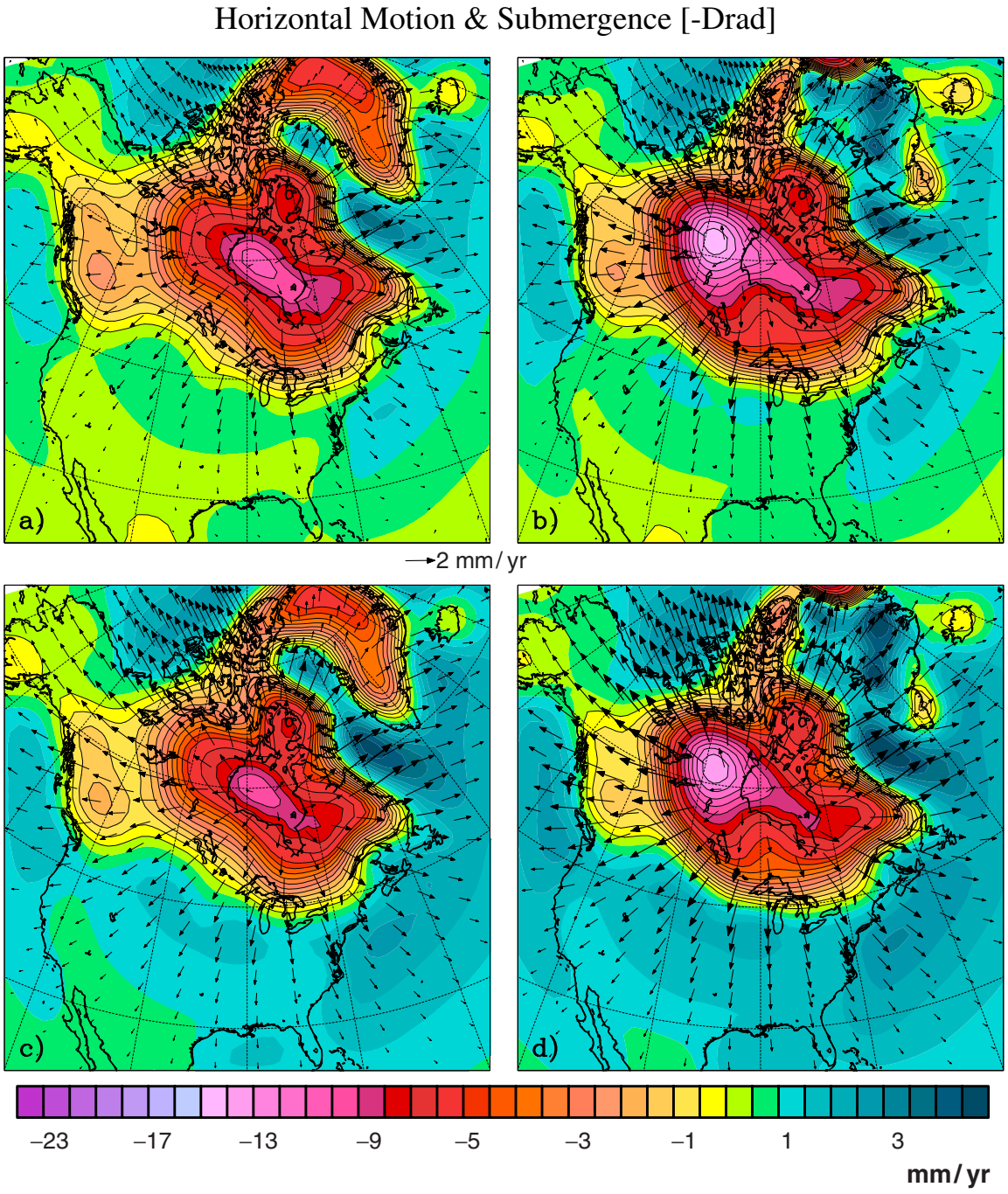

Figure 6 ICE-4G (VM2) and ICE-5GP predictions of the present-day rates of vertical and horizontal motion that should be observed over the regions that were once covered by the Laurentide and Fennoscandian ice-sheets. Vertical motion is shown on the grey scale (a), (b) excluding both the 'broad shelf effect' and rotational feedback and (c), (d) including both of these influences

Very recently Argus *et al.* (1999) have attempted to further test the quality of the ICE-4G (VM2) model by using satellite laser ranging (SLR) and very long baseline interferometry (VLBI) constrained observations of both vertical and horizontal motions at radio telescopes located in both North America and northwestern Europe. Present-day vertical and horizontal rates of displacement of points on the surface of the solid Earth in the Laurentide region that are predicted using the VM2 viscosity model are shown on Fig. 6 for both the ICE-4G and ICE-5GP models of deglaciation. These most recent predictions have been upgraded by including the forcing as a result of the changing centrifugal force, as well as the direct effect resulting from surface loading. For both ICE-4G (VM2) and ICE-5GP (VM2), Fig. 6 shows predictions that both include and exclude the influence of both rotational feed-back and shelf innundation. It is notable that when the latter influences are included the rates of vertical motion and horizontal motion along the USA east coast are somewhat modified. Including this additional forcing modifies the formulae for the vertical and horizontal motion from those in equations (24a) and (24b) in Peltier (1998a) into the following forms

$$U(\theta,\lambda,t)=\sum_{\ell=0}^{\infty}\sum_{m=-\ell}^{+\ell}\left[\frac{4\pi a^3}{(2\ell+1)m_{\mathrm{e}}}\left(L_{\ell m}h_\ell^{E,L}+\sum_{k=1}^{k(\ell)}q_k^\ell\beta_{\ell m}^k\right)\right]Y_{\ell m}+\sum_{\ell=0}^{\infty}\sum_{m=-\ell}^{+\ell}\left[\frac{4\pi}{(2\ell+1)}\frac{1}{g}\left(T_{\ell m}h_\ell^{E,T}+\sum_{k=1}^{k(\ell)}q_k^{'\ell}\beta_{\ell m}^{'k}\right)\right]Y_{\ell m}\quad(8a)$$

$$\underline{V}(\theta,\lambda,t)=\sum_{\ell=0}^{\infty}\sum_{m=-\ell}^{+\ell}\left[\frac{4\pi a^3}{(2\ell+1)m_{\mathrm{e}}}\left(L_{\ell m}\ell_\ell^{E,L}+\sum_{k=1}^{k(\ell)}t_k^\ell\beta_{\ell m}^k\right)\right]\underline{\nabla}Y_{\ell m}+\sum_{\ell=0}^{\infty}\sum_{m=-\ell}^{+\ell}\left[\frac{4\pi}{(2\ell+1)}\frac{1}{g}\left(T_{\ell m}\ell_\ell^{E,T}+\sum_{k=1}^{k(\ell)}t_k^{'\ell}\beta_{\ell m}^{'k}\right)\right]\underline{\nabla}Y_{\ell m}\quad(8b)$$

In equations (8a) and (8b), ''a'', ''m_{e}'' and ''g'' are, respectively, the radius, mass and surface gravitational acceleration of Earth, the $L_{\ell m}$ are the coefficients in the spherical harmonic expansion of the surface mass load L in equation (2), and the $T_{\ell m}$ are the spherical harmonic coefficients in the expansion of the centrifugal potential

$$T(\theta,\lambda,t)=T_{00}Y_{00}(\theta,\lambda)+\sum_{m=-1}^{+1}T_{2\mathrm{m}}Y_{2\mathrm{m}}(\theta,\lambda)\qquad(9)$$

The non-zero coefficients $T_{\ell m}$ are as follows, using results from Dahlen (1976) and neglecting terms of higher order than first in the perturbations ω_{i} to the angular velocity of the Earth Ω_{o} that would obtain in the absence of the GIA effect

$$T_{00}=\frac{2}{3}\omega_3(t)\Omega_{\mathrm{o}}a^2,\qquad(10a)$$

$$T_{20}=-\frac{1}{3}\omega_3(t)\Omega_0a^2\sqrt{4/5},\qquad(10b)$$

$$T_{2,-1}=-(\omega_1+i\omega_2)(\Omega_{\mathrm{o}}a^2/2)\sqrt{2/15},\qquad(10c)$$

$$T_{2,+1}=(\omega_1-i\omega_2)(\Omega_{\mathrm{o}}a^2/2)\sqrt{2/15}.\qquad(10d)$$

In equations (10), the $\omega_{\mathrm{i}}(t)$ are the components of the perturbation to Earth's basic state angular velocity Ω_{o} induced by the glacial isostatic adjustment process. These are computed using the theory described in Peltier (1982) and Wu and Peltier (1984). Because this theory for the rotational response is valid only to first order in the angular velocity perturbations, the expressions for the T_{ij} must also be linearised. In equation (8) the parameters q_k^ℓ, $q_k^{'\ell}$, t_k^ℓ and $t_k^{'\ell}$ are the residues at the poles s_k^ℓ that appear in the viscoelastic normal mode theory of glacial isostatic adjustment of Peltier (1974, 1976, 1985), whereas the $h_\ell^{E,L}$, $h_\ell^{E,T}$, $\ell_\ell^{E,L}$ and $\ell_\ell^{E,T}$ are the elastic asymptotes of the h and ℓ Love number spectra for surface mass (L) and centrifugal potential (T) loading respectively. The functions $\beta_{\ell m}$ and $\beta_\ell^{'m}$ are, as defined in Wu and Peltier (1982),

$$\beta_{\ell m}^k=\int_{-\infty}^{t}L_{\ell m}(t)\mathrm{e}^{-s_k^\ell(t-t')}\mathrm{d}t'\qquad(11a)$$

$$\beta_{\ell m}^{'k}=\int_{-\infty}^{t}T_{\ell m}(t)\mathrm{e}^{-s_k^\ell(t-t')}\mathrm{d}t'\qquad(11b)$$

where the inverse relaxation time spectrum s_k^ℓ for both surface load and potential load forcing is identical so long as the model of the radial viscoelastic structure is the same.

Horizontal motion predictions based upon the first term in equation (8b) were first reported in James and Morgan (1990) and James and Lambert (1993) and later, using more accurate methods to solve the forward problem, in Mitrovica *et al.* (1994) and Peltier (1995, 1998e). In Argus *et al.* (1999) it is noted that although the VLBI vertical motion observations agree that model VM2 may be (slightly) preferred over model VM1 (both models fit most of the data reasonably well), the horizontal motion observations seemed equally clear in their preference for VM1 over VM2 in the sense that they appear to be much slower than predicted by the VM2 model when it is assumed that the predictions both to the northwest and to the southeast of the centre of glaciation in southeast Hudson Bay are of equivalent quality. It is important to note, however, that the original ICE-4G (VM2) model also predicts far too small a rate of vertical motion at the single telescope located in the Northwest Territories to the northwest of Hudson Bay, and that if the ice load were simply increased in thickness or delayed in its melting over the Yellowknife area (where the telescope is located, see Fig. 3a on which the Yellowknife location is denoted YKF), or if the viscosity of the mantle were significantly increased, the vertical motion predicted there (near 0.3 mm yr^{-1} whereas the observation is near 0.8 mm yr^{-1}) would increase and the horizontal motion would decrease. This would apparently have the effect of bringing the predictions of both the vertical and horizontal motion into much closer accord with the observations. Figure 6 shows that the ICE-5GP model does indeed eliminate this misfit to the vertical motion observation at the Yellowknife location. This is an excellent example of the fact that one must be extremely careful as to whether one maps misfits of the theory to the observations into modifications of the radial viscosity profile or into modifications to the glaciation history. Based upon the preceding analysis of Laurentide relaxation times, however, it seems clear that the possibility of improving the model-predicted radial motion for the VLBI site at Yellowknife by increasing the viscosity in the upper part of the lower mantle is untenable. Furthermore, on the basis of the analysis of the far-field LGM depression of eustatic sea-level previously discussed, it is apparent that the ice volume in the ICE-4G model must be increased significantly. It is therefore an interesting issue as to whether the misfit to the VLBI observations at Yellowknife can be eliminated by increasing the ice load in this region (as in ICE-5GP, see below) so as to reconcile the far-field observations of shelf inundation and whether, by modifying the model in this way, the very good fit of the ICE-4G model to the RSL data from the Hudson Bay

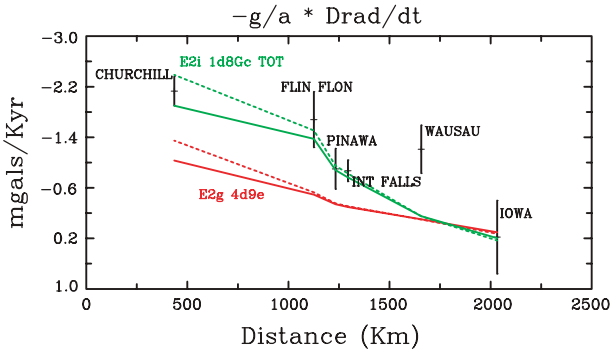

Figure 7 Observations of $\dot{g}$ at the sites shown on Fig. 14, as recently presented in Lambert *et al.* (2001). Theoretical predictions for two different theoretical models are also shown on the figure, namely those for ICE-4G (VM2), denoted E2g, and for ICE-5GP (VM2), denoted E2i. Inspection shows that the approximately factor of two underprediction of $\dot{g}$ at the northern sites delivered by the ICE-4G (VM2) model is entirely corrected by ICE-5GP (VM2), as is the factor of two to three underprediction of the radial motion on the VLBI telescope at Yellowknife

region will be compromised in the process. This is the issue to which I next turn.

As it happens, there now exists a further set of data that may be brought to bear on the plausibility of a Laurentide source for the additional continental ice that appears to be missing from the ICE-4G model. This consists of the set of absolute gravity observations from the region to the south of Hudson Bay (Lambert *et al.*, 2001). Figure 7 shows the Lambert *et al.*, data in the form of inferred values of the time derivative of the surface gravitational acceleration $\dot{g}$ at each of the measurement locations (see Fig. 14 to follow on which the locations are shown at which $\dot{g}$ has been measured). Also shown on Fig. 7 are two sets of model predictions for the $\dot{g}$ traverse, one for the model with the standard ICE-4G distribution of Laurentian land ice and the other for the modified model ICE-5GP which has the substantial increase of ice thickness to the west of Hudson Bay that is required to correct the factor of two to three misfit to the VLBI inference of the radial motion at Yellowknife pointed out in Argus *et al.* (1999) and, clearly, to simultaneously correct the misfit to the $\dot{g}$ observations of Lambert *et al.* (2001). Figure 8 shows the ICE-4G Laurentian

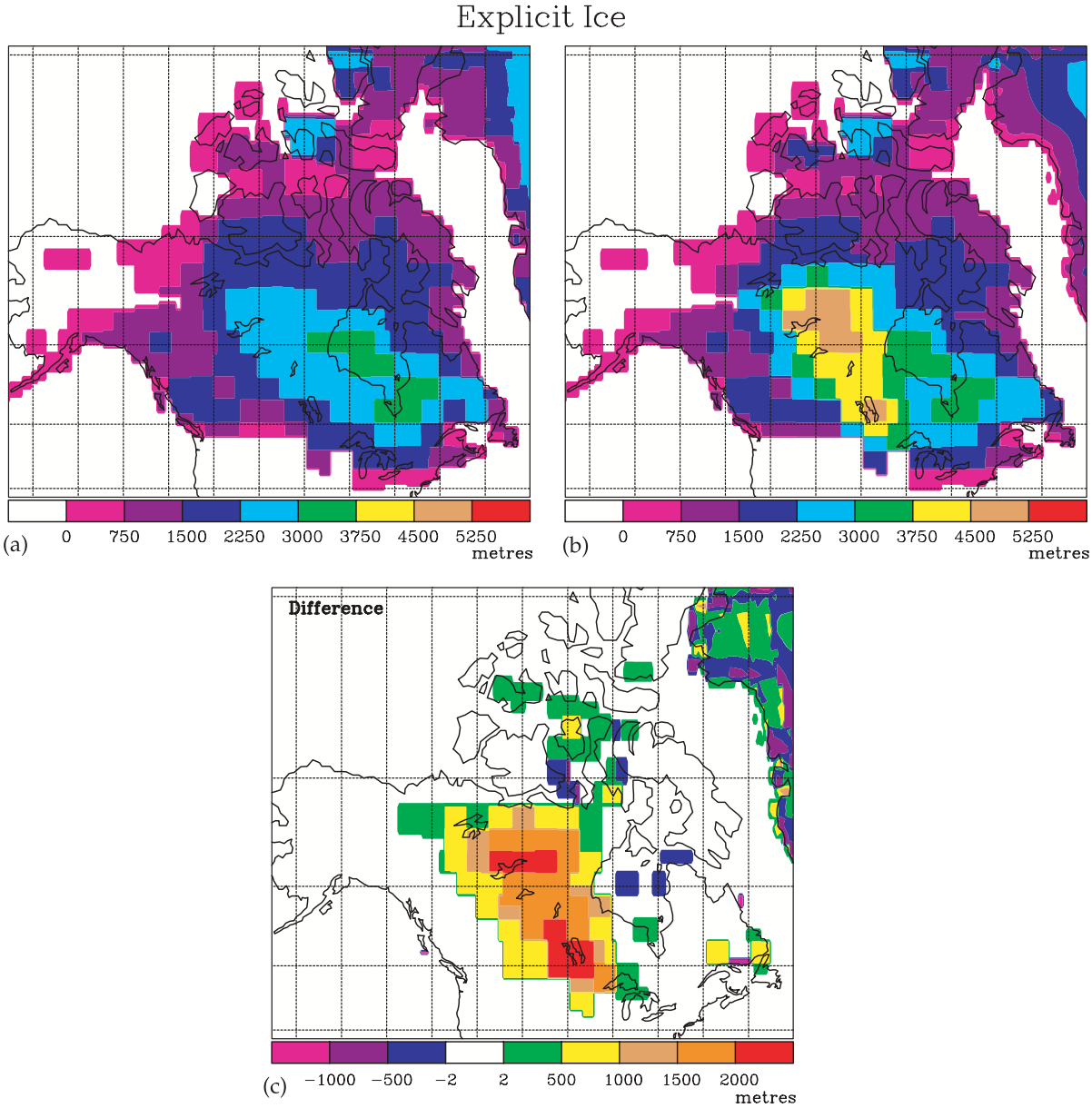

Figure 8 (a) Laurentide ice thickness for the ICE-4G model at LGM, (b) ice thickness for the same region for the ICE-5GP model, (c) the difference in ice thickness over the Laurentian platform between the ICE-4G and ICE-5GP models

ice thickness (a), the increased ice thickness characteristic of ICE-5GP (b) and the difference (c). The increment in ice thickness required to reconcile the model with the observed vertical motion at Yellowknife, as well as the $\dot{g}$ measurements, consists of the introduction of a substantial dome of ice centred over the Yellowknife region and extending to the south and east of this location as a ridge outboard of the southwest portion of Hudson Bay.

The requirement of the VLBI and $\dot{g}$ observations for a substantial enhancement of the thickness of Laurentian ice over the Yellowknife region is not, of course, without resonance in the literature of geomorphology. In fact Dyke and Prest (1987), among others (e.g. see Hillaire-Marcel *et al.*, 1980), have explicitly suggested the existence of a 'Keewatin Dome' of the Laurentide Ice Sheet (LIS) over precisely this region. Their version of the multidomed LIS is shown on Fig. 9, which is reproduced from their paper. I construe the above presented analysis to have firmly established, by a combination of geodynamic and geodetic means, the existence of the Keewatin Dome.

In Lambert *et al.* (2001) it was suggested that the misfit of the standard ICE-3G (VM1) model to their $\dot{g}$ observations could be corrected either by increasing the ice load over their region of observation (to the south of Hudson Bay) or by increasing the viscosity of the mantle from that in VM1 (the VM1 model, a model with upper mantle viscosity of 10^{21} Pa s and lower mantle viscosity of 2×10^{21} Pa s, was suggested by Tushingham and Peltier (1991) and was used by Peltier (1996a) as a first guess in the Bayesian inversion that delivered VM2). I have reproduced the analyses of Lambert *et al.* (2001) using a perturbed version of the VM2 viscosity model coupled to ICE-4G, the results from which are shown on Fig. 10. The alteration of the VM2 radial viscosity profile used for the purpose of these analyses consisted simply of an increase of the viscosity of the entire lower mantle to a uniform value of 4.5×10^{21} Pa s from the value of 2×10^{21} Pa s that is characteristic of VM1 and which is also very close to that in VM2. Inspection of Fig. 10 shows that this increase of the viscosity in the lower mantle does indeed enable the model to fit the data, as Lambert *et al.* (2001) have suggested. Figure 11 demonstrates that an increase in lower mantle viscosity sufficient to reconcile the $\dot{g}$ observations using the original ICE-4G model of the deglaciation process is not compatible with any significant increase in the surface ice load. For the purpose of this further analysis I have used the model of the radial variation of viscosity preferred by Lambeck and co-workers in which the lower mantle viscosity is equal to 10^{22} Pa s. As for the model with lower mantle viscosity of 4.5×10^{21} Pa s, this model fits the $\dot{g}$ observations very well. However, when the additional ice load is introduced, the model grossly overpredicts the $\dot{g}$ observations from the previously ice-covered region.

Based upon the above analyses it therefore seems clear that only the model with the VM2 viscosity profile is acceptable. The logic supporting this conclusion is in fact extremely clear. Firstly, we require significant additional continental ice in the model in order to fit the new constraints on the LGM depression of eustatic sea level provided by the Sunda Shelf and Bonaparte Gulf observations (it is also critical that we can achieve this and remain compatible with the data set from Barbados). Secondly, the viscosity of the upper part of the lower mantle beneath the Laurentian platform cannot be higher than that in VM2, according to the new analyses of Laurentian relaxation times of Peltier (1998a) and Dyke and Peltier (2001), which fix the relaxation time in southeast Hudson Bay to a value near 3.4 kyr (the Lambeck *et al.*, 1996, model, denoted VANU in Fig. 11, predicts a relaxation time for this region greater than 6 kyr). Thirdly, the only plausible region on Earth's surface for the large amount of ice required to effect a reconciliation of the far-field constraints on the LGM eustatic depression of sea-level (ca. 15 m eustatic is required) is the Canadian Shield. Fourthly, only the region to the west of Hudson Bay on this shield can plausibly accommodate the missing mass because the model was entirely unconstrained in this region as (obviously) no relative sea-level curves are available from the continental interior. Finally, and most importantly from a geodynamics perspective, the region to the west of Hudson Bay (Keewatin) can accommodate the required increase in ice mass only if the viscosity of the upper part of the lower mantle is not higher than it is in the VM2 model. I take this sequence of arguments to strongly reinforce the validity of the VM2 model of the radial variation of mantle viscosity.

ICE-4G (VM2) and ICE-5GP (VM2) predictions of geoid-height time dependence: targets for GRACE

Given the solution to equation (1) for the history of relative sea-level change from some time in the past, say LGM, to the present, one may make predictions of a large number of further observations related to the GIA phenomenon. I have mentioned the predictions that one can make concerning observed anomalies in Earth's rotational state, of which the earliest mathematically accurate analyses in the literature are those presented in Peltier (1982, 1983) and Wu and Peltier (1984) for fully compressible models and Sabadini *et al.* (1982) for incompressible models (note that the influence of compressibility on the rotational response to the glaciation–deglaciation process is not at all negligible). These results have since been continually upgraded in accuracy in Peltier (1985, 1988), Mitrovica and Peltier (1993), Peltier and Jiang (1996), Vermeersen and Sabadini (1996) and Peltier (1998e). More recently, Johnston and Lambeck (1999) have reconstructed, and thereby checked the accuracy of, the multi-viscoelastic normal mode solution of Peltier (1982) and Wu and Peltier (1984) and obtained agreement with the inferred value of lower mantle viscosity reported in Peltier (1988, 1996a) and Peltier and Jiang (1996), when the surface load forcing is assumed to be similar. Their preferred model, however, is one in which the viscosity of the entire lower mantle is taken to be much higher than in VM2, a solution which required them to assume that the great polar ice sheets are currently losing mass at a rate sufficient to cause global sea-level to rise at a rate near 1.0 mm yr^{-1}. A model of this kind is entirely untenable for several reasons. Firstly a model of this kind would require that the assumed rapid rise of global sea-level owing to polar ice-sheet melting would have to be assumed to persist over the past 2500 yr in order that the model continue to fit the constraint on the non-tidal acceleration of rotation provided by the analysis of ancient eclipses (e.g. Stephensen and Morrison, 1995) that extend 2500 yr into the past (see discussion in Peltier, 1998a). A sustained rate of sea-level rise over a 2500 yr period at this level would cause global sea-level to rise by 2.5 m, however, and thus eliminate the equatorial highstand of sea-level observed ubiquitously at sites in the far field of the ice sheets (see Peltier (2002a) for a proof of this fact). Secondly, and as demonstrated herein, an increase in viscosity of the entire lower mantle above the value characteristic of VM2 is explicitly ruled out by relaxation times from the Laurentian platform. It is nevertheless important to understand that strong polar ice-sheet melting during the last century may be simply accomodated by the rotational data if

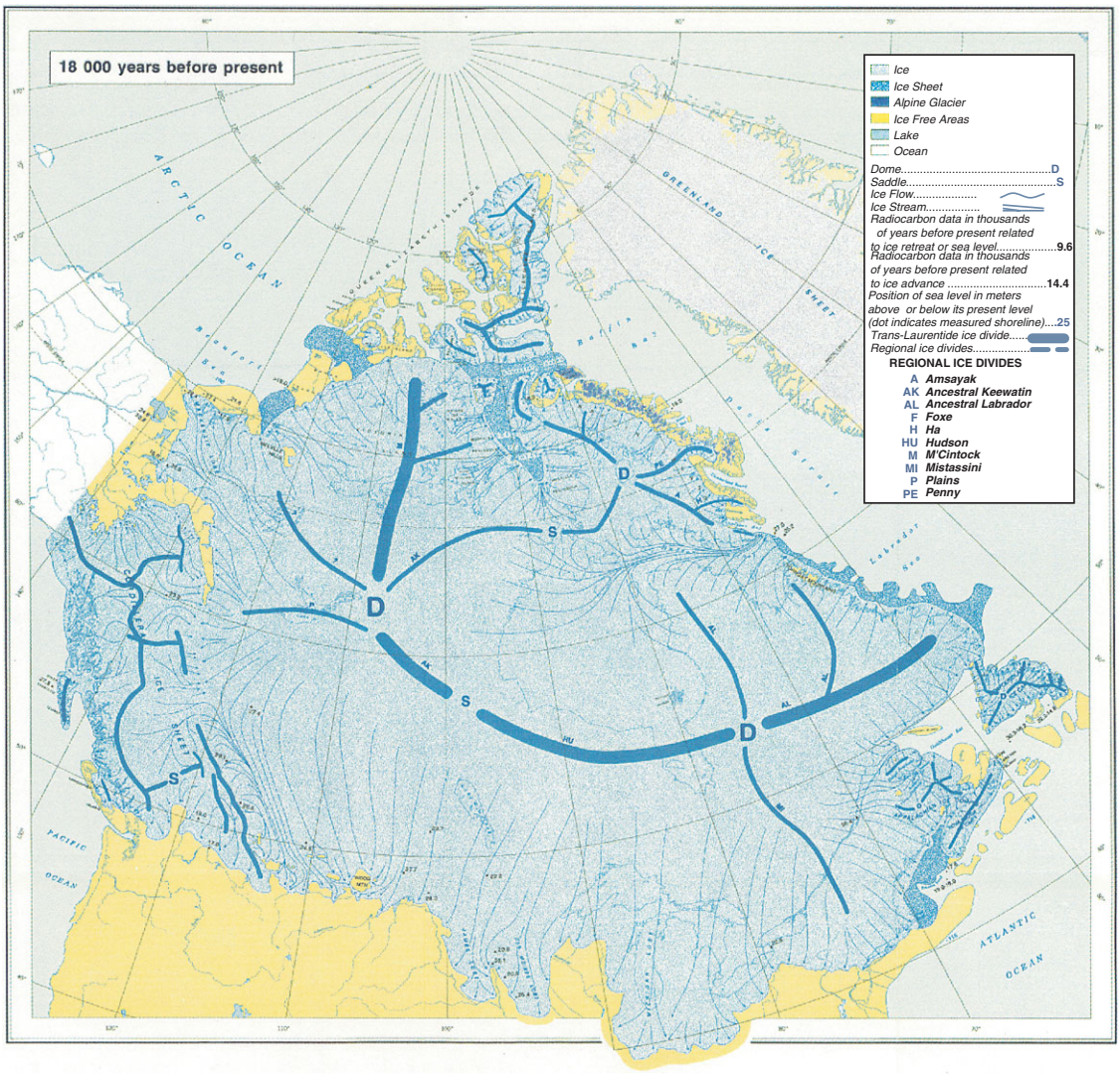

Figure 9 Isopachs of the LGM Laurentide ice sheet according to the geomorphological analyses of Dyke and Prest(1987). Note the hypothesised existence of a Keewatin Dome centred upon Yellowknife in the Northwest Territories of Canada. Note also the implied existence of an intense Hudson Straight ice-stream. It seems clear that it is the existence of such an ice stream that is responsible for preventing the region of maximum Laurentide ice thickness from developing over the Bay itself as it is predicted to do in models that fail to resolve this important dynamic process (e.g. see Tarasov and Peltier, 1999)

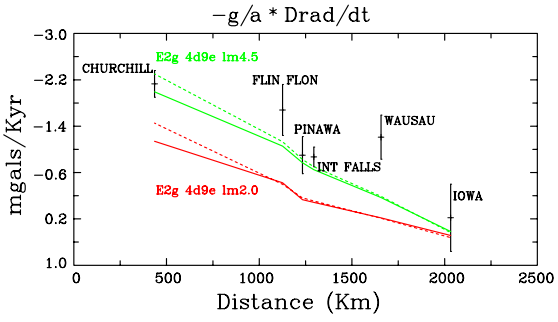

Figure 10 Predictions of $\dot{g}$ at the sites shown on Fig. 14 for both the ICE-4G (VM2) model, denoted by E2g ℓm2.0, and the ICE-4G model with lower mantle viscosity elevated to 4.5×10^{21} Pa s from that in VM2, denoted by E2g ℓm4.5. Clearly the data on $\dot{g}$ may also be fit by simply enhancing the viscosity of the lower mantle and leaving the ice-load distribution in its original single dome over Hudson Bay form

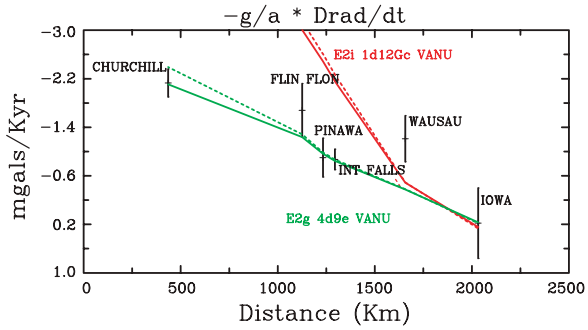

Figure 11 Predictions of $\dot{g}$ at the sites shown on Fig. 14 using the original ICE-4G deglaciation model with the lower mantle viscosity further elevated to the value of 10^{22} Pa s preferred by the ANU group (Lambeck *et al.*, 1990, 1996) denoted by E2g VANU. This model also fits the $\dot{g}$ observations, indicating that for lower mantle viscosity equal to or greater than 4.5×10^{21} Pa s (see Fig. 10) no further significant increase in the $\dot{g}$ prediction obtains. Also shown on this figure is the prediction of the ANU model using the ICE-5GP model of deglaciation denoted E2i VANU. Clearly this model grossly overpredicts $\dot{g}$ and therefore would not allow the increased ice-load required to fit the far-field observations of the LGM eustatic depression of sea-level

the elevation of mantle viscosity is restricted to the lower half of the lower mantle, as shown in Figure 1.

The above referenced increasingly accurate calculations of the rotational response to the glaciation–deglaciation process

have also made it possible to address the question as to whether this process could feed back in any important way on the variations of the solar insolation received by Earth as a result of variations in the geometry of its orbit around the Sun (Peltier and Jiang, 1994; Mitrovica and Forte, 1995; Jiang and Peltier, 1996), the result being that this feed back is suggested to have had a negligible impact on planetary climate over at least the past 3 million years of Earth history. Confirmation of the validity of these analyses has been directly forthcoming through analyses of sedimentary stratigraphy (Lourens *et al.*, 1996). Although Forte and Mitrovica (1997) have suggested that on longer time-scales the influence of the time dependence of the mantle convection process could lead to a significant impact upon climate by significantly modifying the precession constant, and have suggested that a marked effect should have occurred within the most recent 8 million years of Earth history, Pälike and Shackleton (2000) have recently demonstrated that there exists no evidence in the deep-sea sedimentary record for any such effect having occurred.

Of significantly greater importance from the perspective of climate change is the impact of the GIA process upon the observed present-day rate of relative sea-level rise, which many believe to be a consequence of ongoing global warming in the Earth system. In Peltier and Tushingham (1989) it was first shown that this contribution to the secular change of sea-level recorded on modern tide gauge records was large and of global incidence. In order to accurately estimate a mean global rate of relative sea-level rise that could be related to modern climate change, one must therefore 'filter' the tide gauge records so as to eliminate the GIA related bias from the estimate of the secular rate of rise delivered by the data from each gauge. Peltier (1996b) demonstrated that when ^{14}C dated geological measurements of the present-day GIA related rate of RSL rise were used to filter a dense set of tide gauge measured secular sea-level trends from the east coast of the continental USA, and the filtered results were averaged along the coast, an estimate of the regional rate of RSL rise that could be connected to global climate change of ca. 1.9 mm yr^{-1} was obtained for this geographical region. When the ICE-4G (VM2) model is used to filter the same set of tide gauge measurements (Peltier and Jiang, 1997; Peltier, 2001) essentially the same result is obtained. This is of course expected given the fact, previously mentioned in connection with discussion of fig. 23 of Peltier (1998a), that this model of the global GIA process fits the long time-scale ^{14}C dated RSL observations in this region extremely well. Very recent analyses of a globally distributed set of secular sea-level trends measured on tide gauge records of duration exceeding 70 yr have been shown (Peltier, 2001) to deliver an estimate of approximately 1.84 mm yr^{-1} for the mean global rate of sea-level rise, a value that is very close to the estimate derived from USA east coast sites (for further discussion see Douglas and Peltier, 2002). The number of gauges from which such long records are available is severely limited, however, as is the uniformity of the spatial coverage of the oceans that they provide. It therefore remains a serious issue as to how meaningful this inference of the global rate of sea-level rise actually is. There is absolutely no reason to believe that the rate of sea-level rise resulting from global climate change should be uniform over the surface of Earth because each of the known contributions to this effect should themselves induce a rate of rise that is a strong function of geographical position.

Clearly we will be obliged to rely upon satellite based measurement systems to provide the global coverage needed to obtain a definitive result for the globally averaged rate of relative sea-level rise. At present the TOPEX/POSEIDON sea-surface altimeter is the only such system operative and there are significant problems involving the drift of the instrument calibration that must be corrected for in order to infer a global rate of RSL rise. When such corrections are made (e.g. see Nerem *et al.*, 1997a,b; Nerem and Mitchum, 2001) the inferred rate over the single subdecade spanned by the data available is very close to the rate of 2.4 mm yr^{-1} originally inferred on the basis of GIA corrected tide gauge data by Peltier and Tushingham (1989). As surface tide gauge measurements are used to correct for drift of the calibration of the system, however, the measurements are not independent. This is not entirely satisfactory. We will clearly require an extended time series from satellite altimetry that covers many El Niño cycles before data of this kind will be as useful as hoped.

With the launch of the GRACE (Gravity Recovery and Climate Experiment) satellites in early 2002 (March), data will be forthcoming in the form of a measurement, of high accuracy at least to degree and order 32, of the time rate of change of geoid height. As the geoid is, by definition, the equipotential surface that is coincident with the mean level of the sea over the ocean covered portion of the surface of the planet, such a measurement relates directly to the rate of sea-level rise. As is the case with satellite altimetry, this measurement is of the changing level of the sea with respect to the centre of mass of Earth, rather than with respect to the surface of the solid Earth. In order to use the results obtained by solving equation (1) to predict what the GRACE satellite would see in terms of geoid height time dependence, we need to add to a computation of the map of dS/dt for the present day, a prediction of the map of the time rate of change of the local radius of the solid Earth with respect to the centre of mass, say dR/dt. Examples of such analyses were presented previously in Peltier (1998a) and Peltier (1999). Here I will focus firstly upon the form of the signals predicted in this way over the region in which a significant alteration has been proposed to the ICE-4G history of deglaciation and will compare the signals expected on the basis of the ICE-4G (VM2) and ICE-5GP (VM2) models, thus isolating the impact of the radical change in the loading history for the Canadian Prairies advocated herein.

To this end I show first on Fig. 12 the maps of the predicted present-day rate of relative sea-level change for both the ICE-4G and ICE-5GP models of the deglaciation history of Laurentia, as well as the difference. Inspection of this figure makes clear the approximately 2.5 times amplification of the rate of radial displacement that the new model delivers over the Keewatin region to the northwest of Hudson Bay and along the ridge trending to the southeast. It should be understood that this prediction of the time rate of sea-level rise in a region into which the sea never penetrates(!) is to be understood as the time rate of separation of the geoid and the surface of the solid Earth, the former clearly being defined even in the absence of the sea itself by the same value of the gravitational potential as that which defines the surface of the global ocean.

Figure 13 shows the (negative of) the time rate of change of radial displacement predicted by the same two models of Laurentian deglaciation as well as the difference between them. Intercomparison of the fields on Fig. 13, with those for the present-day rate of relative sea-level rise, will show that they are essentially in perfect antiphase, with the surface of the solid Earth rising where relative sea-level is falling. This is a consequence of the fact that in a region undergoing strong post-glacial rebound of the crust owing to the removal of a significant ice load, relative sea-level history is dominated by the crustal rebound signal.

Figure 14 shows the sum of the fields $\dot{S}$ (Fig. 12) and $\dot{R}$ (Fig. 13) and thus the predicted time rate of change of geoid height for the ICE-4G and ICE-5GP models of global deglaciation, models that differ from one another only over the Laurentide platform. Also shown on the geoid height time

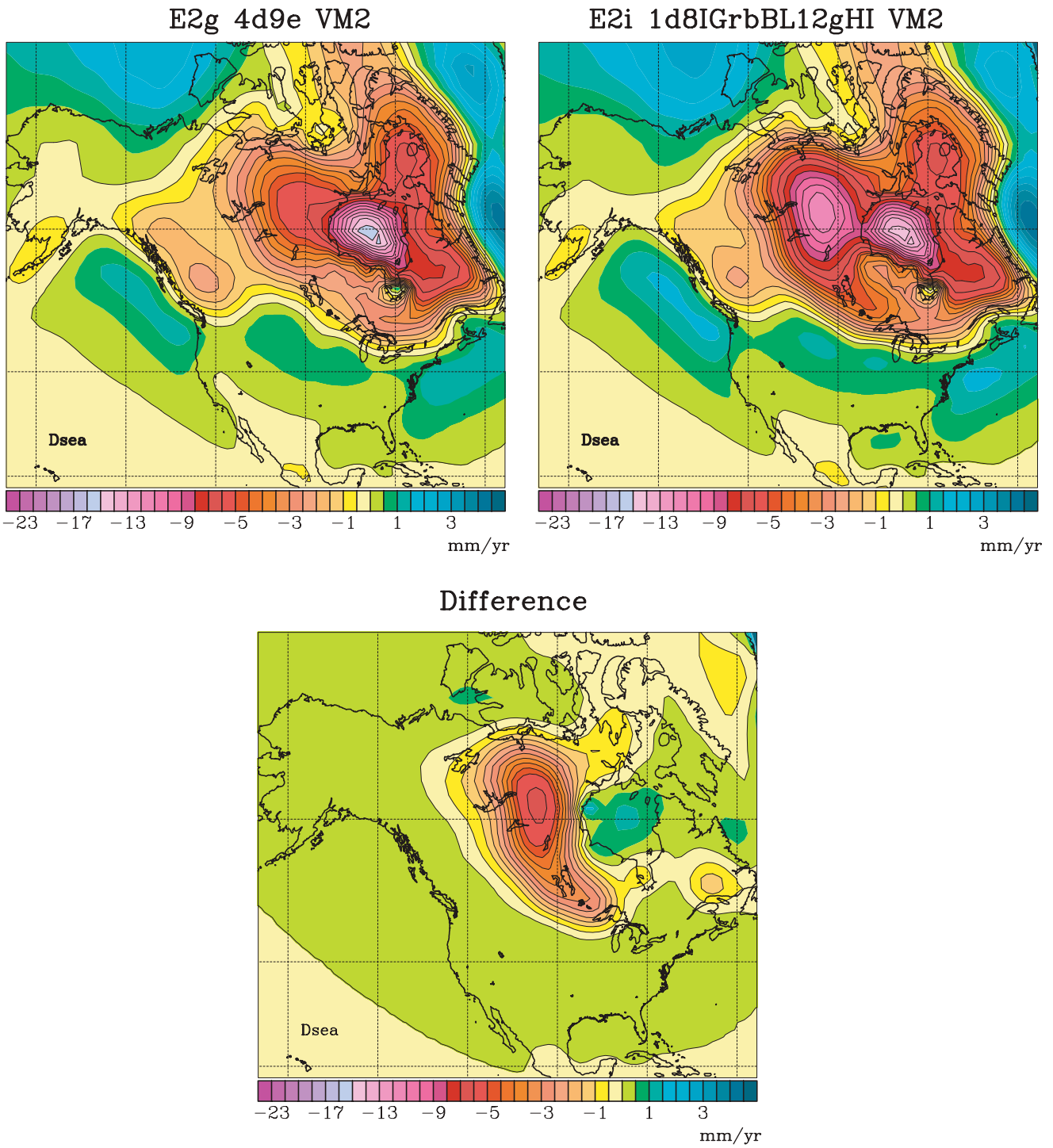

Figure 12 Present-day rate of relative sea-level rise predictions for the ICE-4G (VM2) and the ICE-5GP (VM2) models of the glacial isostatic adjustment process. Also shown is the difference between the predictions of these two models

dependence field for the ICE-4G model are the locations of the sites at which the $\dot{g}$ measurements of Lambert *et al.* (2001) have been made. Comparison of the results for these two models demonstrates that the impact upon the geoid height time dependence signal is large but that it does not prominently exhibit the presence of the second dome of the ice sheet as do the fields $\dot{S}$ and $\dot{R}$ separately. Rather, the impact of the enhanced unloading to the northwest of Hudson Bay causes the single maximum over Canada to extend significantly to the northwest. What we expect to see in the GRACE observations over Laurentia, therefore, is a single 'bulls-eye' of amplitude near 1 mm yr^{-1} that is centred approximately over the Hudson Bay region but which extends over the prairies and Northwest Territories. This is the most intense signal that should obtain over the entire surface of the planet that is associated with the process of continuing glacial isostatic adjustment. A major contribution of this paper is that this signal, once observed, will allow us to obtain confirmation of the existence of the Keewatin Dome.

The expected global pattern of geoid height time dependence will also be of considerable interest in the context of the interpretation of forthcoming GRACE measurements. Figure 15 shows, in Mollweide projection, the theoretical predictions of $\dot{S}$, $\dot{R}$ and their sum, the time dependence of geoid height, for the standard ICE-4G (VM2) model. Evident by inspection of these results is that we expect that the field of geoid height

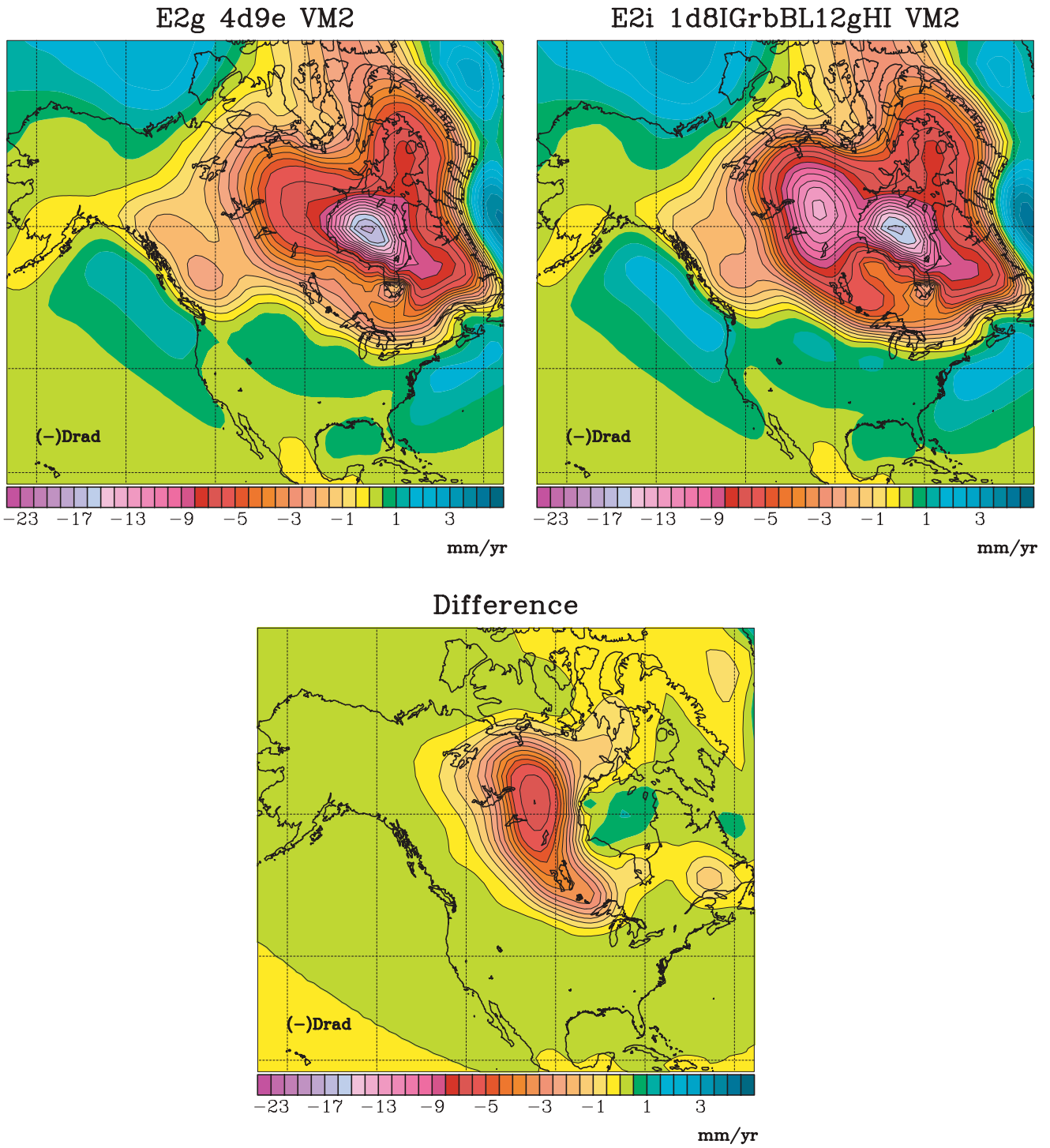

Figure 13 Predictions of the present-day rate of radial displacement for models ICE-4G (VM2) and ICE-5GP (VM2). Also shown is the difference between these predictions. Note that these radial displacement rate calculations are plotted as the negative of the actual field so that one may simply note the strong correlation between $\dot{S}$ and $-\dot{R}$

time dependence should be dominated by a pattern of spherical harmonic degree 2 and order 1 that is the result of the strong impact of polar wander upon this signal. That it is the polar wander component of the rotational response to the isostatic adjustment process that is responsible for this will be evident on the basis of the formulae for the T_{2-1} and T_{2+1} components of the centrifugal potential forcing in equations (10c) and (10d). This update of the continuing effort to compute the geoid height time dependence by including the influence of rotational forcing, a first edition of which appeared in Peltier (1999), has recently been very briefly discussed in Douglas and Peltier (2002). Because the average of the predicted geoid height time dependence over the surface area of the oceans delivers a value of -0.3 mm yr^{-1}, it will be clear that the forthcoming GRACE result for the global rate of sea-level rise that could result from modern climate change will be significantly biased downwards. This bias will have to be removed in order to reveal the impact on sea-level of the influence of modern climate change.

It will be clear based upon the existence of the strong degree 2 and order 1 component of the time rate of change of geoid height signal that is predicted by the global theory of the glacial isostatic adjustment process, due to the influence of true polar wander, that it would be extremely valuable

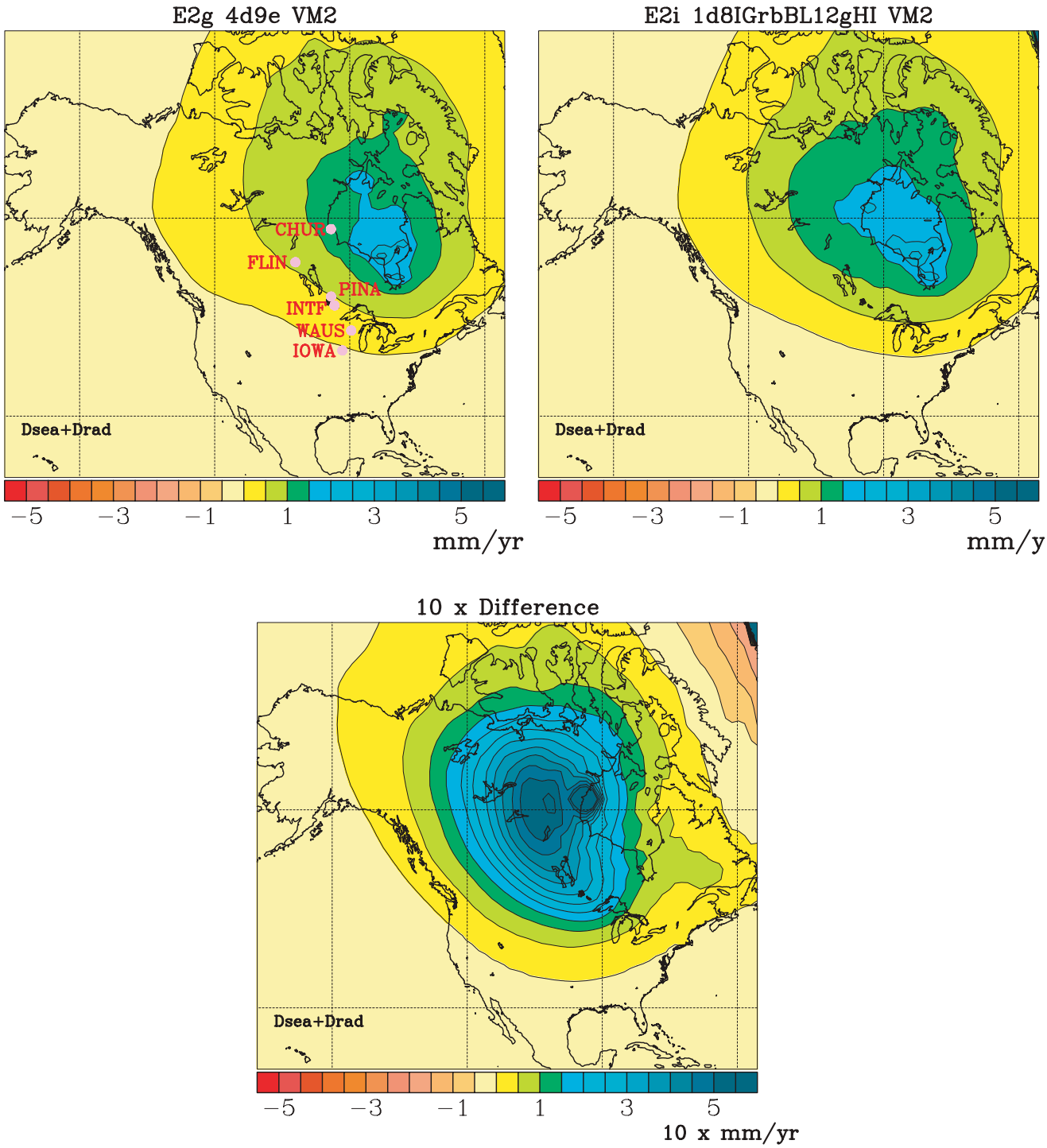

Figure 14 Predictions of the time dependence of geoid height for models ICE-4G (VM2) and ICE-5GP (VM2) obtained by summing the fields $\dot{S}(\theta, \lambda)$ and $\dot{R}(\theta, \lambda)$. Also shown is the difference between these two predictions of geoid height time dependence

if it were possible to obtain independent evidence that the strength of this contribution to the response is indeed as strong as that predicted by the ICE-4G(VM2) model. A means by which this might be accomplished is suggested by virtue of the fact that one of the 4 maxima of the degree 2 and order 1 pattern is located in southernmost Argentinian Patagonia. Although relative sea level observations from this region were missing until recently, Peltier and Drummond (2002) have provided an initial analysis of a newly available set of such data from Rostami *et al.* (2000) stressing the contribution to their interpretation due to the influence of continental shelf exposure and inundation which is included in the model using the method for the incorporation of time dependent ocean function introduced by Peltier (1994). In Fig. 16, I show the results of a further analysis of an important subset of these data which demonstrates the extent to which rotational feed back is important to their interpretation. On this figure the RSL measurements are compared at 8 southern Pategonian sites to the predictions of 4 versions of the Sea Level Equation; respectively a version which includes neither the broad shelf effect of Peltier and Drummond (2002), nor the influence of glaciation pre-history prior to the LGM, nor the influence of rotational feed back. This result is shown as the blue curves on each frame of the Figure. The green curves add the influence of the broad shelf effect to the Patagonian calculations. As discussed in Peltier and Drummond (2002)

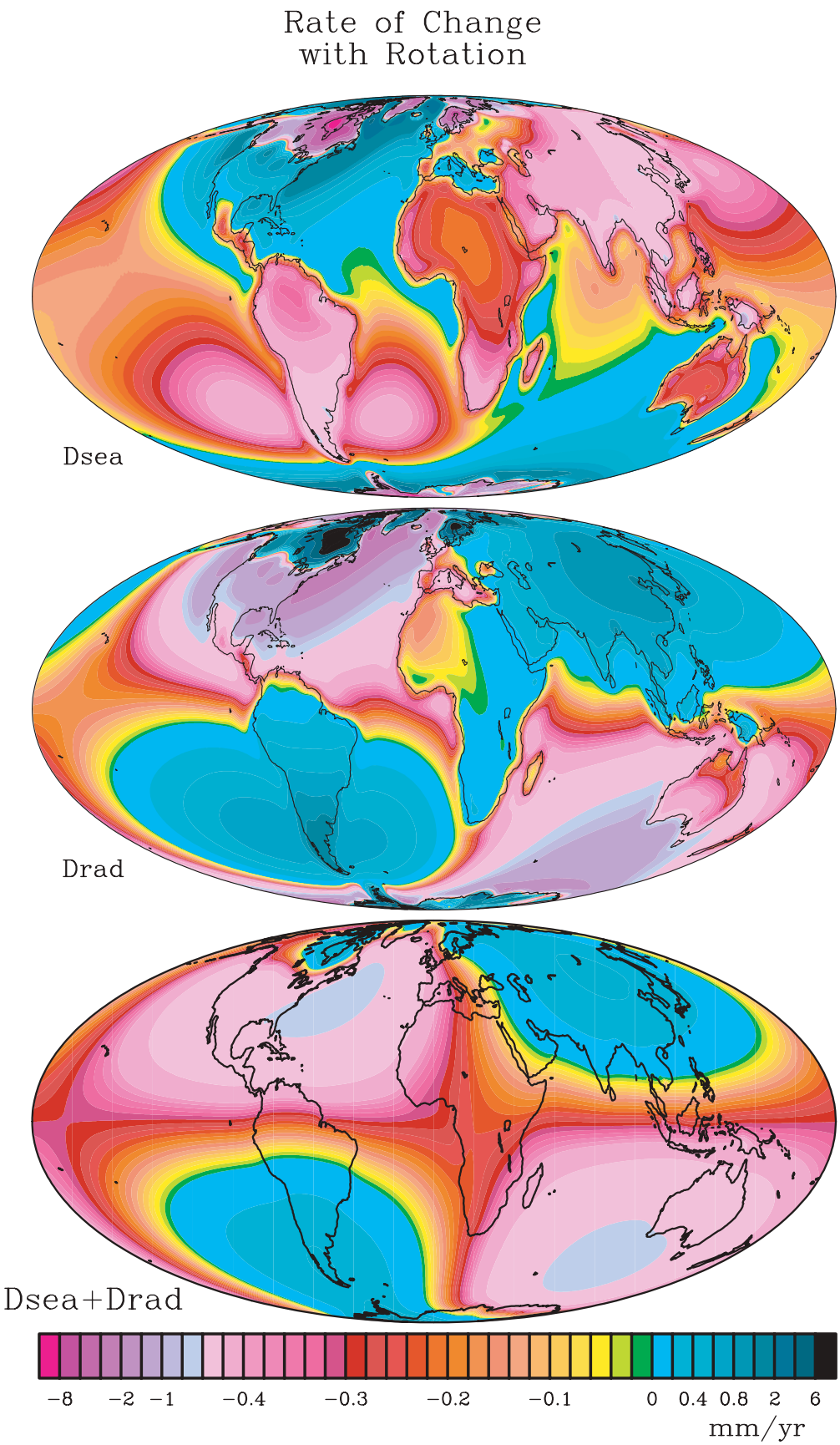

Figure 15 (a) Mollweide projection of the present-day rate of relative sea-level rise made using the standard ICE-4G (VM2) model of the glacial isostatic adjustment process with rotational feed-back included. (b) Same as (a) but for the predicted present-day rate of radial displacement including the influence of rotational feed-back. (c) Present-day geoid height time dependence predicted using the ICE-4G (MV2) model including the full impact of rotational feed-back. The field in (c) is the sum of the fields in (a) and (b)

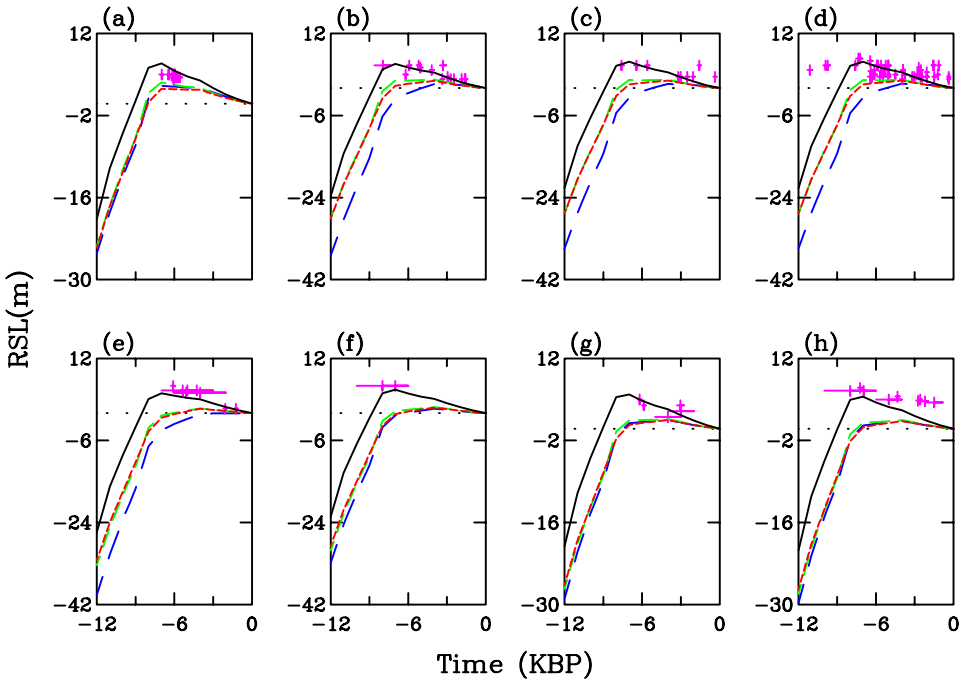

Figure 16 Intercomparisons between theoretical predictions of Holocene relative sea level history at 8 locations along the coast of Argentinian Patagonia. A location map for these sites is provided in Rostami *et al.* (2000) and Peltier and Drummond (2002). On each frame, the (Embedded image moved to file: pic28145.pcx)C dated sea levels (with age corrected to calendar years) are shown as the crosses. The 4 different colour coded curves in each frame correspond to the following suite of models, respectively: (blue) simple ICE-4G(VM2) with no shelf effect, no glaciation pre-history and no rotational feed back, (green) including only the influence of the broad shelf effect, (red) including both the broad shelf effect and glacial pre-history, and finally, (black) including the influence of all of (1) the broad shelf effect, (2) glacial prehistory and (3) the influence of rotational feed back. The sites for which these intercomparisons are shown are (a) Gualeguay, (b) B. Samborombon, (c) Pedro Luro, (d) Rio Colorado, (e) Caleta Valdes, (f) B. Bustamante, (g) Comodoro Rivadavia and (h) Caleta Olivia

this influence is highly significant, although at all of the sites for which comparisons are shown this influence is insufficient to allow the model to fit the data. The amplitude of the mid-Holocene sea level highstand is seriously underpredicted. The red curves correspond to results for which the further effect of glaciation pre-history is included and demonstrate that at these locations this influence is negligible. The final black curves on each frame add the final influence of rotational feed back. Inspection of the individual frames in this figure will show that this influence is as strong as that due to the broad shelf effect at many locations and suffices to enable the ICE-4G(VM2) model to deliver excellent fits to the observations. This further confirms the high quality of this model. Again, geomorphological observations of late Quaternary sea level history have been shown to contribute profoundly to the validation of a model of global geodynamics.

Conclusions

In the past 25 yr, theoretical understanding of the glacial isostatic adjustment process has advanced considerably as has our appreciation of the very wide range of issues on which this subject impinges (see Peltier (1998a) for a recent comprehensive review). As space-geodetic measurement techniques have similarly advanced over this period, including satellite laser ranging (SLR), very long baseline interferometry (VLBI) and, more recently, the global positioning system (GPS) and satellite altimetry, it has become increasingly apparent that, from the point of view of its global incidence, the glacial isostatic adjustment process is becoming increasingly visible to all such systems. It is therefore becoming possible to observe the dynamic evolution of the shape of Earth in real time with sufficient accuracy that we may separate effects as a result of plate tectonics from effects owing to glacial isostatic adjustment. The paper by Argus *et al.* (1999) provides a very clear demonstration of the ability of combined SLR and VLBI measurements to directly observe the latter effect. Real further progress will depend upon the incorporation of GPS measurements into this mix, and global results from such further analyses will be presented elsewhere. The incorporation of SLR measurements into the mix of constraints used to infer both vertical and horizontal motions is especially important as these data make it possible to strongly constrain the origin of the frame of reference of the measurements. As effort in this area continues, further refinement of the ICE-4G (VM2) model undoubtedly will be required. Indeed, several anomalies have been clearly revealed by the intercomparisons of theory and observations discussed herein and are currently being used to further improve the model. These improvements will be further discussed elsewhere.

The most important modification that we have been obliged to make to the model in order to correct misfits of predictions to the observations has concerned the ice-thickness distribution over the Laurentide platform. Recently published far-field constraints on the LGM depression of eustatic sea-level have strongly suggested that the ICE-4G (VM2) model has too little ice. The VLBI and SLR constraints on the upwards radial motion of the surface of the solid Earth on the Canadian Shield well to the west of Hudson Bay have demonstrated that the model-predicted rate was approximately a factor of three lower than observed. This misfit was confirmed by $\dot{g}$ measurements to the southwest of Hudson Bay on a traverse across the USA–Canada border. To correct all of these misfits, I have shown herein that it is necessary to insert into the model of LGM ice thickness a distinct 'Keewatin Dome' of

ice centred over the region of Yellowknife in the Northwest Territories. This correction of the misfits is viable only if the radial profile of mantle viscosity is fixed to the VM2 model. Models of the radial profile of mantle viscosity in which the viscosity of the upper part of the lower mantle is significantly higher than in VM2, such as those preferred by Lambeck and colleagues (e.g. Lambeck *et al.*, 1990, 1996), are strongly ruled out by the analyses discussed herein, as they always have been, based solely upon the relaxation times that characterise the post-glacial rebound of the Laurentian platform.

References

Andrews JT, Falconer G. 1969. Late glacial and postglacial history and emergence of the Ottawa Islands, Hudson, N.W.T.: evidence on the glaciation of Hudson Bay. *Canadian Journal of Earth Science* **6**: 1263–1276.

Argus DF, Peltier WR, Watkins MM. 1999. Glacial isostatic adjustment observed using Very Long Baseline Interferometry and satellite laser ranging geodesy. *Journal of Geophysical Research* **104**: 29 077–29 093.

Bard E, Hamelin B, Fairbanks RG, Zindler A. 1990. Calibration of the ^{14}C timescale over the past 30,000 years using mass spectrometric U–Th ages from Barbados corals. *Nature* **345**: 405–409.

Butler SL, Peltier WR. 2000. On scaling relations in time-dependent mantle convection and the heat transfer constraint on layering. *Journal of Geophysical Research* **105**: 3175–3208.

Butler SL, Peltier WR. 2002. The thermal evolution of the Earth: Models with time dependent layering of mantle convection which satisfy the Urey ratio constraint. *Journal of Geophysical Research*, June.

Clark JA, Farrell WE, Peltier WR. 1978. Global changes in postglacial sea level: a numerical calculation. *Quaternary Research* **9**: 265–287.

Dahlen FA. 1976. The passive influence of the oceans upon the rotation of the Earth. *Geophysical Journal of the Royal Astronomical Society* **46**: 363–406.

Douglas BD, Peltier WR. 2002. The puzzle of global sea level rise. *Physics Today* March: 35–40.

Dyke AS, Prest VK. 1987. Late Wisconsian and Holocene history of the Laurentide Ice Sheet. *Geog. Phys. Quat.* **41**: 237–264.

Dyke AS, Peltier WR. 2001. Forms, response times and variability of relative sea level curves, glaciated North America. *Geomorphology* **32**: 315–333.

Dyke AS, Andrews JT, Clark PU, England JM, Miller GM, Shaw J, Veillette JJ. 2002. The Laurentide and Innuitian Ice Sheets during the Last Glacial Maximum. *Quaternary Science Reviews* **21**: 9–31.

Dziewonski AM, Anderson DL. 1981. Preliminary reference Earth model. *Physics of the Earth Planetary Interiors* **25**: 297–356.

Fairbanks RG. 1989. A 17,000-year glacio-eustatic sea level record: Influence of glacial melting rates on the Younger Dryas event and deep-ocean circulation. *Nature* **342**: 637–641.

Farrell WE. 1972. Deformation of the Earth by surface loads. *Reviews in Geophysics Journal of the Royal Astronomical Society* **10**: 761–797.

Farrell WE, Clark JA. 1976. On postglacial sea level. *Geophysical Journal of the Royal Astronomical Society* **46**: 647–667.

Forte AM, Mitrovica JX. 1996. New inferences of mantle viscosity from joint inversion of long-wavelength mantle convection and post-glacial rebound data. *Geophysics Research Letters* **23**: 1147–1150.

Forte AM, Mitrovica JX. 1997. A resonance in the Earth's obliquity and precision over the last 20 Myr driven by mantle convection. *Nature* **390**: 676–680.

Hanebuth T, Statteger K, Grootes PM. 2000. Rapid flooding of the Sunda Shelf: a late glacial sea level record. *Science* **288**: 1033–1035.

Hillaire-Marcel C, Grant DR, Vincent J-S. 1980. Comment on 'Keewatin Ice Sheet—Re-evaluation of the traditional concept of the Laurentide Ice Sheet'. *Geology* **October**: 466–468.

James TS, Lambert A. 1993. A comparison of VLBI data with the ICE-3G glacial rebound model. *Geophysics Research Letters* **20**: 871–874.

James TS, Morgan WJ. 1990. Horizontal motions due to post-glacial rebound. *Geophysics Research Letters* **17**: 957–960.

Jiang X, Peltier WR. 1996. Ten million year histories of obliquity and precession: the influence of the ice-age cycle. *Earth and Planetary Science Letters* **139**: 17–32.

Johnston P, Lambeck K. 1999. Postglacial rebound and sea level contributions to the geoid and the Earth's rotation axis. *Geophysics Journal International* **136**: 537–558.

Lambeck K, Johnston P, Nakada M. 1990. Holocene glacial rebound and sea-level change in NW Europe. *Geophysics Journal International* **103**: 451–468.

Lambeck K, Johnston P, Smither C, Nakada M. 1996. Glacial rebound of the British Isles III: constraints on mantle viscosity. *Geophysics Journal International* **125**: 340–354.

Lambert A, Courtier N, Sasegawa GS, Klopping F, Winester D, James T, Liard JO. 2001. New constraints on Laurentide postglacial rebound from absolute gravity measurements. *Geophysics Research Letter* **28**: 2109–2112.

Lourens LJ, Antonarakou A, Hilgen FJ, Van Hoof AAM, Vergnaud-Grazzini C, Zachariasse WJ. 1996. Evaluation of the Plio-Pleistocene astronomical timescale. *Paleoceanography* **11**: 391–413.

Martinec Z. 2000. Spectral-finite element approach to three dimensional visco-elastic relaxation in a spherical earth. *Geophysics Journal International* **142**: 117–141.

McConnell RK. 1968. Viscosity of the mantle from relaxation time spectra of isostatic adjustment. *Journal of Geophysical Research* **73**: 7089–7105.

Mitrovica JX, Forte AM. 1995. Pleistocene glaciation and the Earth's precession constant. *Geophysics Journal International* **121**: 21–32.

Mitrovica JX. 1996. Haskell [1935] revisited 1996. *Journal of Geophysical Research* **101**: 555–569.

Mitrovica JX, Peltier WR. 1991. On postglacial geoid subsidence over the equatorial oceans. *Journal of Geophysical Research* **96**: 20 053–20 071.

Mitrovica JX, Peltier WR. 1993. Present-day secular variations in the zonal harmonics of the Earth's geopotential. *Journal of Geophysical Research* **98**: 4509–4526.

Mitrovica JX, Davis JL, Shapiro II. 1994. A spectral formalism for computing three dimensional deformations due to surface loads, 2, Present-day glacial isostatic adjustment. *Journal of Geophysical Research* **241**: 519–520.

Mitrovica JX, Forte AM, Simons M. 2000. A reappraisal of postglacial decay times from Richmond Gulf and James Bay. *Geophysics Journal International* **142**: 783–800.

Munk WH, MacDonald GF. 1960. *The Rotation of the Earth.* Cambridge University Press: New York.

Nerem RS, Mitchum GT. 2000. Observations of sea level change from satellite altimetry. In *Sea Level Rise*, Douglas BC, Kearney MS, Leatherman SP (eds). Academic Press: San Diego: 121–163.

Nerem RS, Haines BJ, Hendricks J, Mitchum JF, White WB. 1997a. Improved determination of global mean sea level variations using TOPEX/Poseidon altimeter data. *Geophysical Research Letters* **24**: 1331–1334.

Nerem RS, Rachlin KE, Beckley BD. 1997b. Characteristics of global mean sea level variations observed by TOPEX/Poseidon using empirical orthogonal functions. *Survey Geophysics* **18**: 293–302.

Pälike H, Shackleton NJ. 2000. Constraints on astronomical parameters from the geological record for the past 25 Myr. *Earth and Planetary Science Letters* **182**: 1–14.

Peltier WR. 1974. The impulse response of a Maxwell Earth. *Review of Geophysics* **12**: 649–669.

Peltier WR. 1976. Glacial isostatic adjustment, II, The inverse problem. *Geophysical Journal of the Royal Astronomical Society* **46**: 669–706.

Peltier WR. 1982. Dynamics of the ice-age Earth. *Advances in Geophysics* **24**: 1–146.

Peltier WR. 1983. Constraint on deep mantle viscosity from LAGEOS acceleration data. *Nature* **304**: 434–436.

Peltier WR. 1985. The LAGEOS constraint on deep mantle viscosity: Results from a new normal mode for the inversion of viscoelastic relaxation spectra. *Journal of Geophysical Research* **90**: 9411–9421.
Peltier WR. 1988. Global sea level and Earth rotation. *Science* **240**: 895–901.
Peltier WR. 1994. Ice age paleotopography. *Science* **265**: 195–201.
Peltier WR. 1995. VLBI baselines from the ICE-4G model of postglacial rebound. *Geophysics Research Letters* **22**: 465–468.
Peltier WR. 1996a. Mantle viscosity and ice-age ice sheet topography. *Science* **273**: 1359–1364.
Peltier WR. 1996b. Global sea level rise and glacial isostatic adjustment: an analysis of data from the east coast of North America. *Geophysics Research Letters* **23**: 717–720.
Peltier WR. 1998a. Postglacial variations in the level of the sea: Implications for climate dynamics and solid earth geophysics. *Reviews in Geophysics* **36**: 603–689.
Peltier WR. 1998b. Implicit ice in the global theory of glacial isostatic adjustment. *Geophysics Research Letters* **25**(21): 3955–3958.
Peltier WR. 1998c. Global glacial isostatic adjustment and coastal tectonics. In *Coastal Tectonics*. Geological Society Special Publication 146, Geological Society Publishing House: Bath; 1–30.
Peltier WR. 1998d. The inverse problem for mantle viscosity. *Inverse Problems* **14**: 441–478.
Peltier WR. 1998e. A space geodetic target for mantle viscosity discrimination: horizontal motions induced by glacial isostatic adjustment. *Geophysics Research Letters* **25**: 543–546.
Peltier WR. 1999. Global sea level rise and glacial isostatic adjustment. *Global Planetary Change* **20**: 93–123.
Peltier WR. 2002a. On eustatic sea level history: Last Glacial Maximum to Holocene. *Quaternary Science Reviews* **21**: 377–396.
Peltier WR. 2002b. Comments on the paper of Yokoyama *et al*. (2000) entitled 'Timing of the last glacial maximum from observed sea level minima'. *Quaternary Science Reviews* **21**: 409–414.
Peltier WR. 2001. Global glacial isostatic adjustment and modern instrumental records of relative sea level history. In *Sea Level Rise*, pp. Douglas BC, Kearney MS, Leatherman SP (eds). Academic Press: San Diego; 65–95.
Peltier WR, Andrews JT. 1976. Glacial isostatic adjustment, I, the forward problem. *Geophysical Journal of the Royal Astronomical Society* **46**: 605–646.
Peltier WR, Jiang X. 1994. The precession constant of the Earth: variations through the ice-age. *Geophysics Research Letters* **21**: 2299, 2302.
Peltier WR, Jiang X. 1996. Glacial isostatic adjustment and Earth rotation: refined constraints on the viscosity of the deepest mantle. *Journal of Geophysical Research* **101**: 3269–3290. (Correction, 1997. *Journal of Geophysical Research* **102** 10 101–10 103).
Peltier WR, Jiang X. 1997. Mantle viscosity, glacial isostatic adjustment and the eustatic level of the sea. *Surveys of Geophysics* **18**: 239–277.
Peltier WR, Tushingham AM. 1989. Global sea level rise and the greenhouse effect: might they be connected? *Science* **244**: 806–810.
Peltier WR, Shennan I, Drummond R, Horton B. 2002. On the glacial isostatic adjustment of the British Isles and the shallow viscoelastic structure of the Earth. *Geophysics Journal International* **148**: 443–475.
Peltier WR, Drummond R. 2002. A 'broad shelf effect' in the global theory of postglacial relative sea level history. *Geophysical Research Letters*, April 15.
Rostami K, Peltier WR, Mangini A. 2000. Quaternary marine terraces, sea level changes and uplift history of Patagonia, Argentina: comparisons with predictions of the ICE-4G (VM2) model of the global process of glacial isostatic adjustment. *Quaternary Science Reviews* **19**: 1495–1525.
Sabadini R, Yuen DA, Boschi E. 1982. Polar wander and the forced responses of a rotating, multilayered, viscoelastic planet. *Journal of Geophysical Research* **87**: 2885–2903.
Shackleton NJ. 2000. The 100,000-year ice-age cycle identified and found to lag temperature, carbon-dioxide, and orbital eccentricity. *Science* **289**: 1897–1902.
Stephenson ER, Morrison LV. 1995. Long-term fluctuations in the Earth's rotation: 700 B.C. to A.D. 1990. *Philosophical Transcations of the Royal Society of London, Series A* **351**: 165–202.
Stuiver M, Reimer PJ. 1993. Extended ^{14}C data base and revised CALIB 3.0 ^{14}C age calibration program. *Radiocarbon* **35**: 215–230.
Tarantola A, Valette B. 1982. Inverse problems = quest for information. *Journal of Geophysics* **50**: 159–170.
Tarasov L, Peltier WR. 1999. The impact of thermo-mechanical ice-sheet coupling on a model of the 100 kyr ice-age cycle. *Journal of Geophysical Research* **104**: 9517–9545.
Tushingham AM, Peltier WR. 1991. ICE-3G: a new global model of late Pleistocene deglaciation based upon geophysical predictions of post-glacial relative sea level change. *Journal of Geophysical Research* **96**: 4497–4523.
Tushingham AM, Peltier WR. 1992. Validation of the ICE-3G model of Würm–Wisconsin deglaciation using a global data base of relative sea level histories. *Journal of Geophysical Research* **97**: 3285–3304.
Tromp J, Mitrovica JX. 1999. Surface loading of a viscoelastic planet—III. Aspherical models. *Geophysics Journal International* **140**: 425–441.
Vermeersen LLA, Sabadini R. 1996. Significance of the fundamental mantle relaxation mode in polar wander simulations. *Geophysics Journal International* **127**: F5–F9.
Wieczerkowski K, Mitrovica JX, Wolf D. 1999. A revised relaxation-time spectrum for Fennoscandia. *Geophysics Journal International* **139**: 69–86.
Wu P. 1998. Postglacial rebound modelling with power-law rheology. In *Dynamics of the Ice Age Earth: a Modern Perspective*, Wu P (ed.). Translation of Technical Publications, Uetikon: Zurich; 365–382.
Wu P. 1999. Modelling postglacial sea levels with a power law rheology and a realistic ice model in the absence of ambient tectonic stress. *Geophysics Journal International* **139**: 691–702.
Wu P, Peltier WR. 1984. Pleistocene deglaciation and the Earth's rotation: a new analysis. *Geophysical Journal of the Royal Astronomical Society* **76**: 202–242.
Wu P, Ni Z, Kauffman G. 1998. Postglacial rebound with lateral heterogeneities: from 2D to 3D modelling. In *Dynamics of the Ice Age Earth: a Modern Perspective*, Wu P (ed.). Translation of Technical Publications, Uetikon: Zurich; 557–581.
Yokoyama Y, Lambeck K, de Dekkar P, Johnston P, Fifield LK. 2000. Timing of the last glacial maximum from observed sea-level minima. *Nature* **406**: 713–716.

